Nanotechnology, Science and Applications

Dovepress
Taylor & Francis Group

Open Access Full Text Article

ORIGINAL RESEARCH

Evaluation of the Effect of Formulation Composition and Physicochemical Properties of Omeprazole and Bisoprolol Hemifumarate on Electrospun Nanofibers Characteristics

Justyna Srebro[1,2], Ewelina Łyszczarz[1], Witold Brniak[1], Dorota Majda[3], Aleksander Mendyk[1]

[1]Department of Pharmaceutical Technology and Biopharmaceutics, Faculty of Pharmacy, Jagiellonian University Medical College, Cracow, Lesser Poland Voivodeship, Poland; [2]Doctoral School of Medicinal and Health Sciences, Jagiellonian University Medical College, Cracow, Lesser Poland Voivodeship, Poland; [3]Department of Chemical Technology, Faculty of Chemistry, Jagiellonian University, Cracow, Lesser Poland Voivodeship, Poland

Correspondence: Ewelina Łyszczarz, Faculty of Pharmacy, Jagiellonian University Medical College, Medyczna 9 St, Cracow, 30-688, Lesser Poland Voivodeship, Poland, Email ewelina.lyszczarz@uj.edu.pl

Purpose: Electrospinning enables the formation of nanofibers by elongating a polymer solution droplet in a high-voltage electrostatic field. The drug substance incorporated into nanofibrous matrix exhibits unique dissolution characteristics, modifiable by polymers selection. The physicochemical properties of the drug substance may also influence structural and functional attributes of the nanofibers. This study aimed to produce nanofibers loaded with small-molecule drugs – omeprazole (OMZ) and bisoprolol hemifumarate (BIS) to investigate how drug and polymer properties influence fiber formation and drug release. The effect of compression into minitablets on dissolution parameters was also assessed.

Methods: Ethanolic solutions of Eudragit® RL (ERL), Eudragit® RS (ERS), and polyvinylpyrrolidone (PVP) were mixed in 13 combinations. OMZ or BIS was dissolved in each mixture and electrospun. Selected nanofibers were compressed into minitablets. Nanofiber morphology, diameter, drug crystallinity and content uniformity were assessed. Dissolution profiles and release kinetics were evaluated for nanofibers and minitablets.

Results: Nanofibers morphology depended on the API and polymers composition. The BIS fibers were nanosized, while OMZ fibers showed heterogeneous thicknesses ranging from 0.54 µm to 5.7 µm. The drug substances were amorphous in nanofibers. OMZ formulations exhibited a sustained release except OMZ_PVP fibers, which released OMZ immediately. The BIS-loaded nanofibers demonstrated a rapid and nearly complete drug release, except for the BIS_ERL+ERS_7+3 formulation, which exhibited prolonged release. Compression of fibers into minitablets preserved the sustained drug release for both drug substances.

Conclusion: The study proves that nanofibers based on Eudragit RL/RS and PVP can be obtained by the electrospinning method. BIS properties such as good solubility, balanced hydrophobic-lipophilic nature, surface charge, and amorphous form contributed to its rapid release, unlike OMZ.

Keywords: electrospinning, minitablets, drug delivery, polymers, sustained-release, release kinetics, amorphization

Introduction

Electrospinning is a method of producing solid fibers from a droplet of polymeric solution by applying an electrostatic voltage. The polymer solution in a volatile solvent is fed from a syringe to a needle connected to a high-voltage generator using a syringe pump. Under the applied voltage, the charges in the solution differentiate, and those with the same sign as the needle accumulate on the solution's surface. With increasing voltage, the charges begin to repulse each other expanding the droplet and changing its shape into a Taylor cone. When electrostatic repulsion overcomes surface tension, a jet is formed. The stretched jet undergoes whipping, during which the solvent evaporates. The resulting fibers solidify on the surface of the collector.[1–3]

Received: 18 April 2025
Accepted: 8 July 2025
Published: 28 July 2025

In recent years, electrospinning has gained increasing interest in pharmaceutical sciences and biomedical applications. Examples of its use are the development of formulations with small molecule drugs, nucleic acids, or proteins, formulations for diagnosis and imaging, or tissue engineering.[4–6] Compared to other methods for obtaining micro- and nanofibers, such as self-assembly or phase separation, electrospinning is characterized by a relatively simple and low-cost preparation and a wide choice of materials with potential applications.[5,7] The fibers obtained in the electrospinning process are characterized by high porosity and high surface area. Furthermore, the morphology, mechanical properties and drug release rate from these fibers can be easily modified by the process parameters and polymers used.[5,8] In the case of poorly soluble drug substances, electrospinning is an efficient method to produce amorphous solid dispersions.[9] The literature reviews indicate that for nanofibers containing small-molecule drugs, the most common biodegradable polymers used are polycaprolactone (PLC), polylactic acid (PLA), polylactic-co-glycolic acid (PLGA), polyvinyl alcohol (PVA), chitosan or non-biodegradable grades of Eudragit characterized by pH-dependent dissolution (Eudragit L100/S100).[1,2,4–6,8,10,11]

Eudragit polymers (polymethacrylates) are extensively used in pharmaceutical technology due to their versatility and broad range of applications. Due to their excellent film-forming properties, Eudragit polymers are used for taste masking or coating of pH-targeted solid oral dosage forms. In addition, they can be used as matrix-forming excipients; thus, their potential use in other dosage forms is still being explored. The properties of polymethacrylates (polymers of acrylic and methacrylic acid or its esters) result from the type-specific quantitative ratio of selected functional groups. Interesting examples are Eudragit RL and RS, which are pH-independent and insoluble polymers.[12,13] The presence of quaternary ammonium groups in the form of chloride salts that dissociate in aqueous media makes them water-permeable and swellable. Additionally, the quaternary ammonium groups are ionized at all pH levels of the gastrointestinal tract, making the drug release from Eudragit RL and RS pH-independent. The difference between Eudragit RL and RS is that the former contains more ammonium moieties and, therefore, is more swellable than the latter. RL and RS grades of Eudragit have been applied in the development of prolonged- or controlled-release formulations.[10,13,14]

The use of Eudragit RL and RS in electrospinning has been also investigated. Eudragit RS was used to obtain nanofibers containing corticosteroids: methylprednisolone acetate, and triamcinolone acetonide[15,16] In the case of methylprednisolone acetate, the faster release was achieved from microfibers than from the crude drug substance.[15] Interestingly, nanofibers containing triamcinolone acetonide were characterized by a slower release of the therapeutic substance.[16] With the use of Eudragit RS and S blends, fibers with indomethacin dedicated for colonic drug delivery were obtained.[17] Other nanofibrous formulations based on Eudragit RL and RS include nanofibers dedicated to ocular administration,[18] gastro-retentive nanofibers[19] and thermoresponsive nanofibers.[20]

Although electrospinning is a promising technique for continuous manufacturing, it still presents significant challenges in downstream processing.[1,6,21–23] The most intuitive route of nanofiber administration is in the form of orodispersible films.[24,25] However, such application requires uniformity of drug dispersion and proper stability of the fibers during storage. On the other hand, compressing nanofibers into tablets on an industrial scale appears to be a far more complex and costly process. The low bulk density, poor flowability, and delicate structure make it impossible to compress nanofibers continuously without proper preprocessing.[22] Szabó et al[23] successfully produced 600 mg tablets containing fibers with itraconazole. They developed a continuous process comprising milling, feeding, mixing, and tableting of the fibers, which could be further scaled up.[23] In another study, the effect of cellulose nanofibers (CNFs), as a potential drug carrier, on the properties of orodispersible tablets was investigated. The addition of CNFs slightly reduced the flowability of the tablet mass, yet provided adequate tablet disintegration time and sufficient hardness compared to tablets prepared with other excipients.[26] The tableting capabilities of nanofibers have also been studied on a laboratory scale, resulting in tablets with meloxicam,[27] acetaminophen,[28] or theophylline.[29] Several attempts have also been made to manufacture minitablets from nanofibers.[30,31]

Poller et al[30] obtained minitablets by direct compression of nanofibers based on PVP and prednisolone. The minitablets were characterized by fast disintegration and immediate release of the drug substance. As a result of electrospinning, prednisolone was transitioned to an amorphous form, and nanofibers showed stability up to 10 months of storage.[30] Nakamura[31] studied the properties of minitablets containing cellulose nanofibers and acetaminophen prepared using different compression forces. The minitablets containing 20% or more CNF had similar immediate release profiles, independent of the compression force used.[31] The development of the minitablets is beneficial as they are

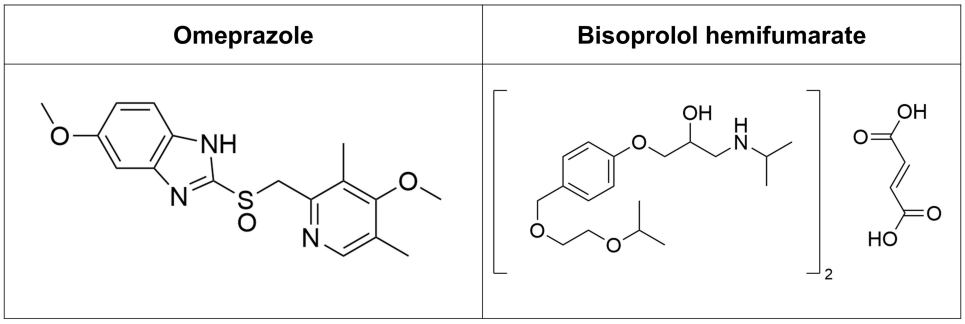

Figure 1 Chemical structures of omeprazole and bisoprolol hemifumarate.

suitable for various patient groups, including pediatric patients.[32] The high acceptability of orodispersible minitablets, even higher in comparison to glucose syrup, has been shown in neonates.[33] An unquestionable advantage of minitablets is that the dose can be easily and precisely adjusted according to the patient's needs due to the small doses of the drug in a single minitablet.[34] In the case of pediatric formulations, it is also beneficial to reduce the frequency of drug administration, which can be achieved with sustained-release formulations.

The examples of therapeutic substances used in pediatric therapy are omeprazole (OMZ) and bisoprolol hemifumarate (BIS) (Figure 1). To date, little work has been done in the development of minitablets[35,36] or electrospun formulations containing these drug substances. Omeprazole belongs to the group of proton pump inhibitors and is used in the management of gastroesophageal reflux disease (GERD).[37] Bisoprolol fumarate is a selective beta-blocker used in the treatment of hypertension and heart failure.[38] Omeprazole is a lipophilic molecule, which is very slightly soluble in water and sparingly soluble in ethanol.[37,39] A challenge in the development of drug dosage forms with omeprazole is its instability in acidic media.[37] In contrast, BIS is characterized by a balanced hydrophilic-hydrophobic characteristic and is freely soluble in both water and ethanol.[40–42]

Considering the need to develop a dosage form suitable for children and potential applications of the electrospinning technique, the aim of the study was to produce nanofibers containing model small-molecule drugs – OMZ and BIS. Simultaneously, the study aimed to investigate the influence of model drugs with different physicochemical properties and chosen polymers on nanofibers formation and drug delivery characteristics. The fibers obtained were compressed into minitablets to determine the effect of different compression forces on the release profile of drug substances from the polymer matrices.

Polymers chosen for the study were PVP and Eudragit in two different grades, namely RS and RL. PVP, the immediate-release polymer, was combined with sustained-release Eudragit polymers to enhance the dissolution of the drug from the polymeric matrix. To characterize the drug delivery from nanofibers and minitablets, uniformity of content, dissolution, and drug release kinetics studies were conducted. The influence of drug substances and polymers on fibers' morphology was assessed with the use of optical and scanning electron microscopy (SEM). The solid-state properties of OMZ and BIS before and after the electrospinning process were investigated using X-ray diffraction (XRD) and differential scanning calorimetry (DSC).

Materials and Methods

Materials

Bisoprolol hemifumarate (BIS, but-2-enedioic acid; 1-(propan-2-ylamino)-3-[4-(2-propan-2-yloxyethoxymethyl)phenoxy]propan-2-ol, CAS: 104344–23-2) was purchased from Wuhan ChemNorm Biotech Co. Ltd., Wuhan, China. Omeprazole (OMZ, 6-methoxy-2-[(4-methoxy-3,5-dimethylpyridin-2-yl)methylsulfinyl]-1*H*-benzimidazole, CAS: 73590–58-6) was purchased from Hangzhou Jhechem Co. Ltd., Hangzhou, China. The polymers used as fiber matrices were Eudragit RS PO (ERS, Ammonio Methacrylate Copolymer Type B Ph. Eur.) and Eudragit RL PO (ERL, Ammonio Methacrylate Copolymer Type A Ph. Eur.), kindly donated by Evonik Operations GmbH, Darmstadt, Germany and poly(vinylpyrrolidone) (PVP, Kollidon K30) purchased from BASF, Ludwigshafen am Rhein, Germany.

For the high-performance liquid chromatography (HPLC) analysis acetonitrile of gradient grade purity was used. For preparation of other solutions, the following substances of analytical grade were used: diethylamine for HPLC purchased from Chempur (Piekary Śląskie, Poland), formic acid solution purchased from Honeywell (Seelze, Germany), di-sodium hydrogen phosphate anhydrous purchased from POCH (Gliwice, Poland), sodium hydroxide microgranules purchased from Witko (Łódź, Poland), potassium dihydrogen phosphate (Emsure® ISO) purchased from Merck KGaA (Darmstadt, Germany), and ethanol 96% (v/v). The water used for the studies was produced by an Elix 15UV Essential Reverse Osmosis System (Merck KGaA, Darmstadt, Germany).

Methods

Electrospinning Process

The solutions for the electrospinning process were prepared by dissolving polymers ERL, ERS, and PVP in ethanol 96% (v/v). The solutions were stirred continuously at 350 rpm using Heidolph MR HeiTec magnetic stirrer (Schwabach, Germany). The concentrations of the polymeric solutions were determined based on the preliminary studies. Obtained ethanolic solutions of Eudragit RL PO 25% (w/w), Eudragit RS PO 25% (w/w), and PVP 40% (w/w) were subsequently mixed in different proportions. OMZ was added to the matrix solutions to reach the concentration of 2% (w/w) and stirred with a glass rod until completely dissolved. Prepared solutions were immediately electrospun. In a subsequent step, the same formulations were reconstituted with the addition of BIS. Table 1 shows the composition of the formulations used in the electrospinning process.

Table 1 Composition of the Formulations with Omeprazole (OMZ) or Bisoprolol Hemifumarate (BIS) Used for the Electrospinning Process

Name of the Formulation	OMZ [%]	BIS [%]	ERL Solution [%]	ERS Solution [%]	PVP Solution [%]
OMZ_ERL	2	–	98	–	–
OMZ_ERS	2	–	–	98	–
OMZ_PVP	2	–	–	–	98
OMZ_ERL+ERS_3+7	2	–	29.4	68.6	–
OMZ_ERL+ERS_1+1	2	–	49	49	–
OMZ_ERL+ERS_7+3	2	–	68.6	29.4	–
OMZ_ERL+PVP_3+7	2	–	29.4	–	68.6
OMZ_ERL+PVP_1+1	2	–	49	–	49
OMZ_ERL+PVP_7+3	2	–	68.6	–	29.4
OMZ_ERS+PVP_3+7	2	–	–	29.4	68.6
OMZ_ERS+PVP_1+1	2	–	–	49	49
OMZ_ERS+PVP_7+3	2	–	–	68.6	29.4
OMZ_ERL+ERS+PVP_1+1+1	2	–	32.6	32.7	32.7
BIS_ERL	–	2	98	–	–
BIS_ERS	–	2	–	98	–
BIS_PVP	–	2	–	–	98
BIS_ERL+ERS_3+7	–	2	29.4	68.6	–
BIS_ERL+ERS_1+1	–	2	49	49	–

(*Continued*)

Table 1 (Continued).

Name of the Formulation	OMZ [%]	BIS [%]	ERL Solution [%]	ERS Solution [%]	PVP Solution [%]
BIS_ERL+ERS_7+3	–	2	68.6	29.4	–
BIS_ERL+PVP_3+7	–	2	29.4	–	68.6
BIS_ERL+PVP_1+1	–	2	49	–	49
BIS_ERL+PVP_7+3	–	2	68.6	–	29.4
BIS_ERS+PVP_3+7	–	2	–	29.4	68.6
BIS_ERS+PVP_1+1	–	2	–	49	49
BIS_ERS+PVP_7+3	–	2	–	68.6	29.4
BIS_ERL+ERS+PVP_1+1+1	–	2	32.6	32.7	32.7

The equipment used for the electrospinning process was a syringe pump Ascor AP14 (Ascor Med Sp. z o.o., Warsaw, Poland) and a high-voltage power supply E-Fiber EF020 SKE Research Equipment® (Bollate, Italy). The 20 mL syringe filled with the prepared sample was connected to the disposable 23-gauge stainless steel blunt needle via a silicone connector tube. The applied voltage was 30 kV, and the tip-to-collector distance was 25 cm for all formulated samples. Produced fibers were collected on the aluminum foil wrapped around the stationary collector. The electrospinning process was conducted at ambient temperature and humidity. They ranged from 20°C to 28°C and 40% RH to 61% RH. The syringe feeding rate was set at 2 mL/h for the samples containing BIS and 4 mL/h for OMZ. Collected fibrous mats were stored in a desiccator in sealed aluminum bags.

Morphology Assessment

Obtained fibrous mats were assessed visually and under a polarising microscope (Hund H-600, Wetzlar, Germany). Additionally, the morphology of electrospun fibers was evaluated by scanning electron microscopy (SEM). Uniformly sized samples of the fibrous mats obtained were sputtered with gold and investigated using the Hitachi S-4700 scanning electron microscope (Hitachi High-Tech, Tokyo, Japan) at magnifications of 1000×, 2000×, 5000×, and 10,000×. The applied beam acceleration voltage was 20 kV. The fibers' thickness was estimated from acquired SEM images using scaling tools of CorelDRAW Software (Corel Corp., Ottawa, Canada).

DSC and XRD Studies

The differential scanning calorimetry studies (DSC) of raw active pharmaceutical ingredients (APIs), polymers, and electrospun fibers (formulations chosen for compression) were performed using a Mettler-Toledo DSC 3+ System (Greifensee, Switzerland). In addition, the incompatibilities of the drug substances with each of the polymers, and between the polymers alone were investigated. Physical mixtures of polymers and APIs were based on fiber formulations. Weighed samples containing OMZ and BIS were heated in an argon atmosphere (50 cm^3/min) at temperatures ranging from 20°C to 250°C and from −50°C to 150°C, respectively. The temperature range for the analysis of the polymers alone was 20°C to 250°C. The heating rate used for all measurements was 10°C/min. Measurements were carried out once per sample without replication.

The crystalline structures of prepared samples (excluding polymers) were investigated in X-Ray diffraction analysis (XRD). The analysis was performed using Philips PW1830 X-ray diffractometer (Amsterdam, The Netherlands) equipped with X'Pert Data Collection version 2.0e (PANalytical B.V). Diffraction patterns were collected over a 2θ range between 3° and 43° with a 5°/min step. Measurements were carried out once per sample without replication.

HPLC Analysis

Quantitative analysis of BIS and OMZ was carried out using high-performance liquid chromatography (HPLC). For BIS analysis, a Jasco LC-4000 RHPLC set supported by Jasco ChromNav software (JASCO Corporation, Tokyo, Japan) was

used. The analysis was performed on the Kinetex C18 LC Column (2.6 µm, 100 Å, 100 × 4.6 mm; Phenomenex, USA) at 25°C. Based on the method of Charoo et al,[43] the mobile phase was composed of solution A and acetonitrile in a ratio of 70:30 (v/v).[43] Solution A was composed of 8 mL formic acid and 6 mL diethylamine per 1000 mL of aqueous solution (pH 4.4 ± 0.05). The flow rate was set at 0.25 mL/min, and the injection volume was 5 µL. BIS detection was performed at λ = 223 nm with a retention time of 2.0 min. The total run time for the analysis was 3.0 min. The calibration curve for BIS was linear over the concentration range of 1.0–100.0 µg/mL (R^2 = 0.9998).

OMZ analysis was performed using Agilent Technologies 1260 Infinity HPLC set (Agilent Technologies Inc., California, USA) with a diode array detector and autosampler. The column used for the analysis was InfinityLab Poroshell 120 EC-C18 column (4 µm, 120 Å, 100 × 4.6 mm, Agilent Technologies, USA), thermostated at 25°C. The mobile phase was composed of phosphate buffer (pH = 7.4 ± 0.05) and acetonitrile 55:45 (v/v) according to the method proposed by Murakami et al.[44] The flow rate was 1 mL/min. The sample injection volume was 5 µL, and the sample detection was set at λ = 300 nm. The OMZ retention time was 1.65 min (total run time 2.5 min). The OMZ calibration curve was linear over the concentration range of 2.0–30.0 µg/mL (R^2 = 0.9997).

Quantitative analysis was performed in a single replicate for each analyzed sample containing bisoprolol hemifumarate or omeprazole.

Content Studies

Fibrous mats weighed on the analytical scale MS105DU (Mettler Toledo, Greifensee, Switzerland) were transferred to 50 mL flasks and dispersed in a solution composed of 10 mL of ethanol and 20 mL of relevant dissolution medium. The solutions were shaken for 2 h at 375 rpm (Heidolph Unimax 1010 laboratory shaker, Schwabach, Germany). Filtrated samples (nylon syringe filters, 0.22 µm) were analyzed using HPLC. The study was performed in triplicate for all fibers obtained. Based on the results, average content values with standard deviations were calculated and expressed as percentages of the theoretical values.

Dissolution Studies

Dissolution studies for fibers and minitablets were performed in the pharmacopoeial type II (Ph.Eur. 11.8, monograph 2.9.3) paddle apparatus SR8 PLUS with Dissoette II automatic fraction collector (Hanson, Teledyne Labs, California, USA). The studies were conducted at 37°C and in 500 mL of medium for 8 h. The dissolution medium for BIS formulations was water, while for OMZ a phosphate buffer of pH = 7.4. The paddle rotation speed was 50 or 75 rpm, respectively. During the study, Japanese Pharmacopoeia baskets sinkers were used to prevent the flotation of fibrous mats.

Five single minitablets or one piece of fibrous mat of known weight were placed in each vessel of the dissolution apparatus. The samples of 4 mL were collected at 5, 10, 15, 30, 45 min and 1, 2, 4, 8 h of the study. After sampling, the medium was automatically refilled with the same volume to maintain the constant conditions of the dissolution. For each formulation, the tests were performed in triplicate. Obtained samples were analyzed using HPLC, and the results were recalculated based on the API content.

Fibers Compression and Minitablets' Assessment

Two selected fiber formulations were compressed into 3 mm minitablets (MTs) using EZ-SX texture analyzer (Shimadzu, Kyoto, Japan) with a custom-built probe adapted from an EK0 eccentric tablet press. The probe consisted of a single minitablet punch with a diameter of 3 mm attached to the measuring head and die mounted on a flat surface of the measuring table. The maximum load of the measuring head was 500 N.

The formulations selected to prepare minitablets were BIS_ERL+ERS_7+3 and OMZ_ERS+PVP_7+3. The formulations were chosen based on their dissolution profiles and the amount of the API released during the study. The calculated weight of the BIS and OMZ fibers per MT was 13.25 mg and 15.46 mg, respectively, which resulted in a theoretical content of 1 mg of API per minitablet.

A fibrous mat thoroughly weighed on analytical scale MS105DU (Mettler Toledo, Greifensee, Switzerland) was transferred into the probe die using tweezers. The tablet punch moved downward with a constant speed of 10 mm/min.

The applied compression forces for each formulation were 50, 150, 250, and 400 N. The diameter, mass, and thickness of 15 minitablets from each series were measured. Average values and standard deviations were calculated.

Analysis of Release Kinetics

An analysis of the dissolution curves was performed to determine the kinetics of the dissolution process. The analysis was performed using the open-source software RKinetDS.[45] The software allows the resulting dissolution curves to be fitted to known mechanistic or empirical models.

The calculations were performed for all fibers and minitablets containing BIS or OMZ. The models selected for analysis did not include lag time, due to the absence of such a phenomenon in the curves obtained. Particular consideration was given to the Hixon-Crowell, Hopfenberg, Korsmeyer-Peppas, and Peppas-Sahlin models, due to their relevance in characterizing the prolonged release of drug from the polymeric matrix. The first two models suggest an erosion mechanism of the drug release, while the other two suggest diffusion-driven drug release. Calculations were carried out on a minimum of 3 points, excluding 0 and the points for which the drug release exceeded 65%. The root mean squared error (RMSE) values were used to assess and compare the model's predictability.

For formulations where analysis with data cutoff was not possible due to insufficient data points, the analysis was conducted including data points exceeding 65%. This deviation from the standard protocol is noted in the discussion of the results.

Statistical Analysis

For statistical analysis of the study results, OriginPro software v. 9.9.0.220 and MS Excel (Microsoft 365) were used. The statistically significant differences ($p < 0.05$) were calculated using a one-way analysis of variance (ANOVA) with a post hoc Tukey's multiple comparison test.

For statistical comparison of the resulting dissolution profiles, mean dissolution time (MDT) and area under the curve (AUC) were calculated (Excel spreadsheet, Microsoft 365). MDT was determined based on the following equation:[46]

$$MDT = \sum \frac{ti \times \Delta Qi}{Q\infty}$$

t_i – sampling interval [h], ΔQ_i- the amount of API released in the specified time interval [%], Q_∞- the maximum amount of API released [%].

The AUC values of the dissolution curves were calculated using the trapezoidal method, ranging from 0 to 8h.

Correlation of the data was calculated using OriginPro software (v. 9.9.0.220) with the Correlation Plot app (v. 1.31), which calculates Pearson's correlation coefficient and p-values for the selected sets of variables.

Results and Discussion

Electrospinning Process

The electrospinning process resulted in the preparation of 13 batches of fibers containing OMZ and 4 batches containing BIS. The electrospinning process was more efficient for OMZ-containing formulations, which allowed the use of higher flow rate (4 mL/h). In the case of BIS formulations, the flow rate had to be reduced to 2 mL/h. Frequent clogging of the needle, observed during the electrospinning process, additionally contributed to the prolonged processing time of BIS formulations. This phenomenon may have resulted from conducting the electrospinning process under conditions of higher temperature and humidity than for formulations with OMZ. It was proven that rapid evaporation of volatile solvent from a droplet on the surface of a needle can cause its clogging.[47] As the ambient temperature increases, the evaporation rate of ethanol is higher. In another study, it was observed that nanofibers spun from cellulose acetate had a larger diameter when the RH was 45% or more. This might be due to increased precipitation of insoluble cellulose acetate from organic solution through absorption of water from the environment.[48] Excessive needle clogging can also be influenced by applied voltage, solution viscosity, or needle-to-collector distance,[49] but the values of these parameters were constant and/or comparable between formulations with BIS and OMZ during the study. The fibers containing more than 68% of ERL or PVP in the matrix formulation were electrospun more easily than other formulations.

It was found that most of the BIS formulations changed their physical state during storage. They softened and disintegrated. In the case of fibers containing more than 68% of PVP, this phenomenon occurred rapidly, whereas in the formulations with lower amounts of PVP and the BIS_ERS fibers within 48 hours after preparation. This effect was observed despite storage in aluminum bags and in a desiccator. All unstable formulations were excluded from further studies.

Although there is no literature data on interactions between polymers used in the study and bisoprolol fumarate, Marini et al[50] reported the interaction between PVP and atenolol (AT),[50] which, like BIS, belongs to the group of β-blockers and shares a similar aryloxypropanolamine structure. According to Ph. Eur. 11.8., atenolol is sparingly soluble in water, whereas bisoprolol fumarate is very soluble in water.[40,51] Marini et al[50] observed aggregation of AT platelets and PVP particles in the mixture, regardless of exposure to moisture. They also noted interactions between AT and PVP in DSC and XRPD studies and concluded that the observed changes might be caused by the presence of hydration water in PVP.[50]

The phenomenon described for BIS formulations was not observed in fibers containing the very slightly soluble OMZ. Results of the DSC studies show no incompatibilities between BIS and PVP.

Morphology Assessment

The morphology of the electrospun fibers may be affected by many factors, such as process parameters, drug loading, solution properties, or ambient conditions.[8] Therefore, variables such as applied voltage, distance from the needle to a collector, drug loading, solvent dielectric constant, and volatility were kept constant for all formulations to eliminate the influence of additional parameters.

Fiber diameter measurements showed that BIS fibers were nanosized, while 8 of the 13 formulations with OMZ exceeded 1 μm in diameter. The fibers obtained were randomly oriented within the mats and exhibited heterogenous thickness.

The average diameter of OMZ fibers ranged from 540 nm (± 180 nm) for the OMZ_ERS+PVP_7+3 formulation, to 5.7 μm (± 2.2 μm) for OMZ_ERL. BIS fibers' diameter ranged from 530 nm (± 370 nm) for BIS_ERL to 650 nm (± 590 nm) for BIS_ERL+ERS_3+7 fibers. Fiber thickness measurements for all formulations are listed in Table S1.

BIS fibers were characterized by smaller average diameters than the corresponding OMZ fibers. For instance, the diameter of BIS_ERL+ERS_1+1 fibers was 590 nm (± 260 nm), whereas the OMZ_ERL+ERS_1+1 formulation was 1.34 μm (± 0.41 μm). This may result from differences in ambient conditions and flow rates during the electrospinning process. According to the literature reports, the fibers' diameter might decrease with increasing ambient temperature and humidity.[52,53] Increasing the temperature may reduce the viscosity of the solution, and increase the solvent evaporation rate, which results in the formation of thinner fibers.[52] In the study conducted by Park et al[54] it was found that the fibers' diameter increased with the increasing flow rates of the ethanolic solution. High flow rates result in decreased charge density in the jet, which leads to incomplete fiber formation.[54] For BIS-containing fibers, the temperature and relative humidity of the process were slightly higher than for fibers with OMZ. Additionally, the flow rate of BIS spinning solutions was reduced. Together, these factors may have influenced the diameter of BIS fibers. Another reason for the smaller diameter of the BIS fibers may be the salt effect.[55,56] Bisoprolol hemifumarate ionization in the ethanolic-water solution might increase the charge density of the jet and thus elongation forces, which led to the formation of fibers with smaller diameters.

SEM images of BIS_ERL+ERS_3+7 and BIS_ERL+ERS_7+3 fibers are presented in Figures 2a and b. The BIS_ERL +ERS_3+7 fibers were characterized by a more tangled structure and heterogenous diameters (650 nm (± 590 nm)) than the second formulation. A similar effect was observed for OMZ fibers. A predominant amount of ERL over ERS in the formulation improved the fibers' structure by straightening and smoothing their surface (Figure 2c and d).

The OMZ fibers based on ERL and ERS (Figure 2c and d) were thinner than the corresponding formulations with ERL and PVP (Figure 2e and f). The thicknesses of OMZ_ERL+ERS_3+7 (Figure 2c) and OMZ_ERL+ERS_7+3 (Figure 2d) were 950 ± 690 nm and 830 ± 280 nm, whereas of OMZ_ERL+PVP_3+7 fibers (Figure 2e) and OMZ_ERL +PVP_7+3 (Figure 2f) were 1.45 ± 0.7 μm and 1.15 ± 0.5 μm, respectively. The fibers with higher amount of PVP (Figure 2e) were more crumbled, and less uniform than those with lower amount of this polymer (Figure 2f). Higher

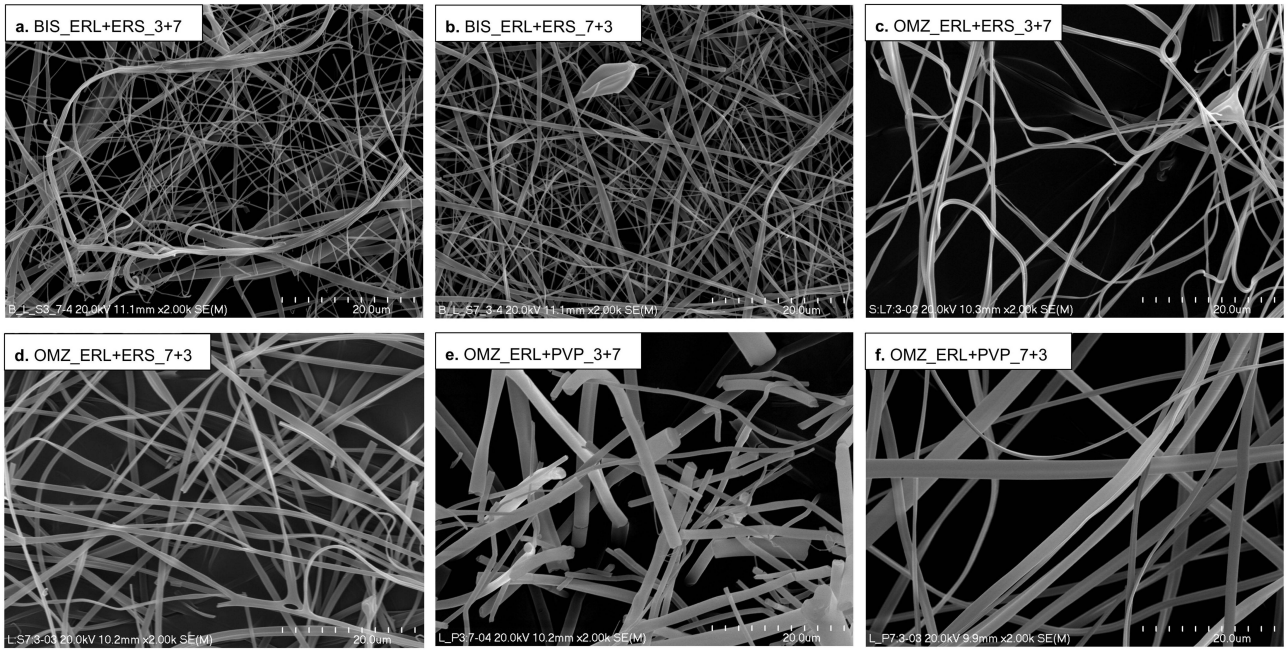

Figure 2 SEM images of BIS (**a** and **b**) and OMZ (**c–f**) fibers (magnification x 2.00k): (**a**) BIS_ERL+ERS_3+7, (**b**) BIS_ERL+ERS_7+3, (**c**) OMZ_ERL+ERS_3+7, (**d**) OMZ_ERL +ERS_7+3, (**e**) OMZ_ERL+PVP_3+7, (**f**) OMZ_ERL+PVP_7+3.

susceptibility of fibers containing PVP to fragmentation was also reported in another paper.[57] Increasing the amount of ERL in the formulation significantly elasticized and smoothed the fiber surfaces, which resembled ribbons (Figure 2f).

In the case of fibers containing PVP, a larger diameter than for Eudragit-based formulations could be expected due to the higher concentration of polymers in the matrix.[58] However, the distribution of fiber diameters was very large, probably due to the low viscosity of obtained solutions. The fibers based on ERS+PVP were thinner in comparison to respective ERL+PVP formulations (Table S1). This might be related to the cationic nature of ERL and ERS. Amarjargal et al[20] and Rošic et al[59] found that cationic charges in the polymer decrease the thickness of the fibers, by increasing elongation forces in the jet.[20,59] Because ERL contains more cationic quaternary ammonium groups, the formation of thinner fibers would be expected. However, the observed results were quite the opposite. As in the case of BIS fibers, the formulation with the most heterogenous fiber diameters was OMZ_ERL+ERS_3+7. This finding confirms the beneficial effect of ERL on fiber structure.

The analysis of the correlation between polymers content and fiber thickness showed moderate effect of Eudragit on thickness (Figure S1). A higher amount of ERL led to an increase in fiber thickness ($r = 0.49$), whereas in the case of ERS, the relationship was inversed ($r = -0.41$). However, both correlations were statistically insignificant ($p > 0.05$). The amount of PVP did not show the relationship with thickness.

The macroscopic observations of the fibrous mats are consistent with the microscopic image of the fibers (Figure S2). It was observed that the fiber brittleness increased with the increasing amount of the ERS in the formulation.[19] The fibrous mats containing ERL instead of ERS were characterized by higher flexibility and smoothness. Increasing the amount of PVP in the matrix to 49% resulted in fluffier but less elastic fibrous mats. Fibers containing the highest amounts of ERL in combination with PVP presented a cotton wool-like structure.

DSC and XRD Studies

The DSC curves of the raw OMZ, neat polymers and electrospun fibers are presented in Figure 3a. The DSC profile of unprocessed OMZ exhibits two distinct thermal events: an endothermic peak with T_{onset} at 156°C corresponding to the melting point of the drug, followed by an exothermic event with T_{onset} at 163°C, which is indicative of thermal degradation and decomposition of the API, as reported in literature.[60] In contrast, the thermograms of the electrospun

https://doi.org/10.2147/NSA.S535362

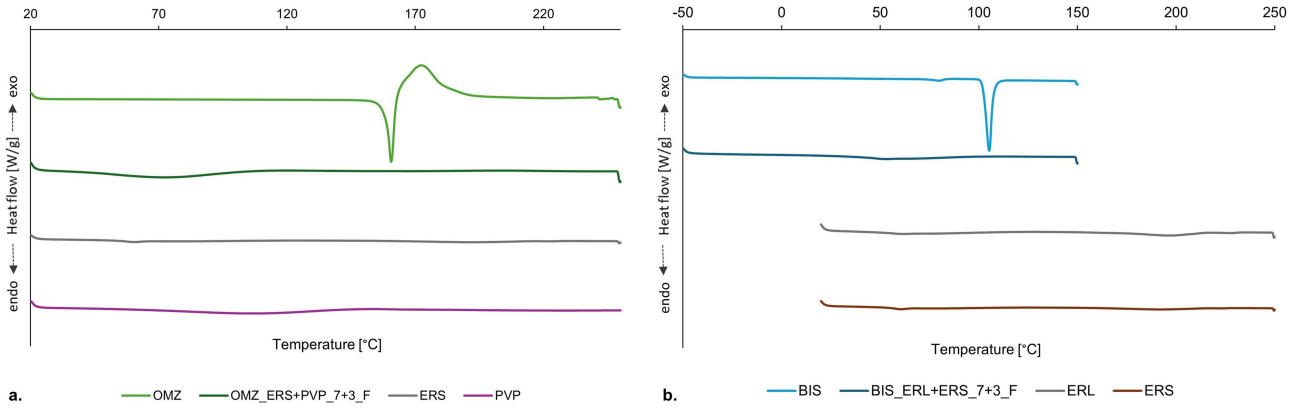

Figure 3 DSC profiles of OMZ (**a**) and BIS (**b**) formulations used for minitablets compression (OMZ, BIS - API in bulk; ERL, ERS, PVP - polymers in bulk; OMZ_ERS+PVP_7+3_F, BIS_ERL+ERS_7+3_F - electrospun fibers).

fibers containing OMZ show no detectable endothermic or exothermic transitions associated with the crystalline form of the drug. This absence of characteristic melting and recrystallization peaks strongly suggests that OMZ underwent complete amorphization during the electrospinning process. Instead, the DSC curves of the fiber formulations display only a single, broad endothermic event with an onset temperature near 45°C, which can be attributed to the evaporation of residual moisture or bound water present in the polymeric matrix. This phenomena may be attributed to the presence of PVP in the polymer matrix. PVP is a hygroscopic polymer known to readily absorb moisture from the environment. In the case of the neat polymer, water evaporation is also observed, as evidenced by the endothermic peak occurring between 57°C and 143°C (Figure 3a). Similar thermal events associated with water loss have also been reported in other studies involving PVP-based formulations.[61,62]

The DSC curve of the raw BIS presented in Figure 3b, reveals two endothermic peaks with T_{onset} at 74°C and 101°C. These thermal events are characteristic of the melting transition associated with the hydrate form of bisoprolol.[63] Consistent with the observations for the OMZ formulations, the DSC thermograms of BIS fibers show no detectable endothermic peaks corresponding to the crystalline form of the drug. The absence of such melting signals confirms the complete amorphization of bisoprolol fumarate. Notably, a slight thermal event observed at approximately 52°C (T_{min}/T_{max}) in the thermogram of the BIS_ERL+ERS_7+3_F formulation corresponds to the glass transition of the Eudragit polymers.[10,14]

Furthermore, the DSC analysis revealed no evidence of physicochemical incompatibilities between the active pharmaceutical ingredients and the polymers used in the formulations. Likewise, no interactions were detected among the polymers themselves. These findings support the thermal and physicochemical stability of the complex formulations obtained.

X-ray diffractometry of the raw API, electrospun fibers, and corresponding physical mixtures was performed to characterize the molecular structure of the drug substances and evaluate the effect of the electrospinning process on their crystallinity.

The analysis of the diffractogram collected for omeprazole (Figure 4a) with the sharp Bragg peaks at 2θ values of 9.13°, 11.13°, 12.21°, 14.71°, 15.71°, 17.09°, 19.21°, 19.59°, 20.35°, 23.81°, 24.63°, 25.67°, and 27.61° indicates that the investigated sample is the Astra Form-A according to patent USOO6150380A.[64] In the case of bisoprolol, the diffraction pattern with sharp Bragg peaks registered at 5.39°, 10.77°, 11.21°, 13.31°, 14.99°, 16.13°, 18.41°, 19.59°, 18.69°, 19.37°, 19.49°, 19.89°, 20.59°, 22.13°, 23.83° and 27.17° (Figure 4b) corresponds to the literature data for I polymorphic form.[63] The different results regarding the polymorphic form of bisoprolol in DSC and XRD studies may be due to the way the analyses were conducted and their sensitivity. Based on these results, we speculate that the bisoprolol that was used for the study was a mixture of two polymorphic forms, ie, form I and hydrate.

As can be seen in Figure 4, the presence of a characteristic amorphous diffractogram for electrospun fibers, regardless of the type of the API confirms that the electrospinning process led to amorphization of both OMZ and BIS. In the case

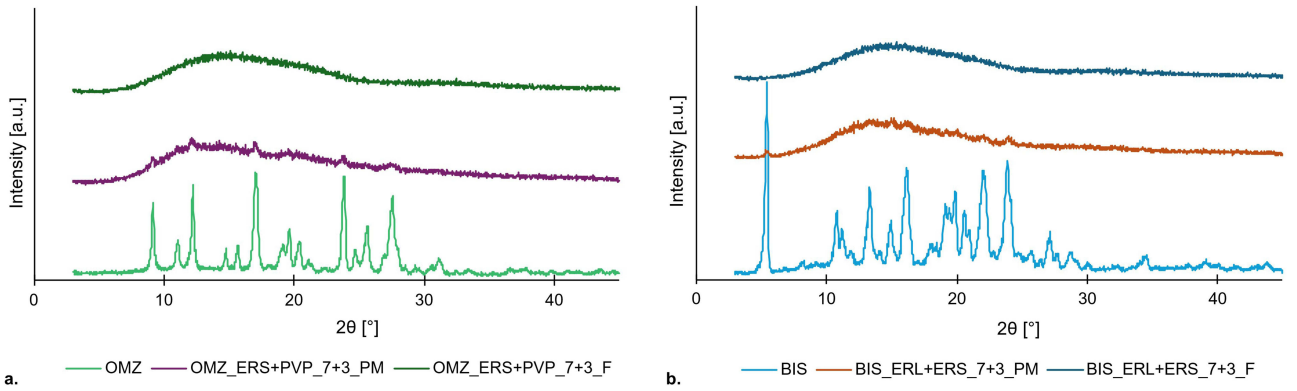

Figure 4 X-ray diffraction patterns of OMZ (**a**) and BIS (**b**) formulations used for minitablets compression (OMZ, BIS - API in bulk; OMZ_ERS+PVP_7+3_PM, BIS_ERL +ERS_7+3_PM - a physical mixture; OMZ_ERS+PVP_7+3_F, BIS_ERL+ERS_7+3_F - electrospun fibers).

of the physical mixture, small Bragg peaks are interposed on the amorphous halo, indicating the presence of these substances in crystalline form. Their low intensity is due to the low API content in the mixture.

Content Studies

For most OMZ fibers, the content of the drug substance was in the range of 99–115% of theoretical values. Only for the OMZ_ERS formulation the determined content was lower and was 78%. This may have been caused by the poorer solubility of omeprazole in the ethanolic solution of ERS, potentially leading to partial sedimentation during the electrospinning process. However, this hypothesis could not be confirmed by instrumental analysis and needs further explanation. The BIS content in fibers was in the range of 98–110%.

Dissolution Studies – Fibers

The dissolution studies were performed for all obtained fibers and minitablets containing OMZ or BIS. Conducted studies focused on the assessment of the influence of the polymer and its concentration on the dissolution behavior of the incorporated APIs.

Among the tested formulations, only OMZ_PVP fibers were completely dissolved during the 8-hour studies. This outcome can be attributed to the excellent water solubility of PVP.[62,65] In contrast, for the other formulations containing water-insoluble polymers, ie, ERL and ERS, a residue remained on the sinker wires.[66] When ERL predominated in the formulation, the insoluble residue formed a rubbery, elastic mass. In the case of ERS, the residue was brittle and disintegrated immediately under slight pressure.

Omeprazole

The results of the dissolution studies for OMZ fibers are presented in Figures 5–8 and Table S2. The OMZ formulations were characterized by prolonged release of the drug substance, except for OMZ_PVP, which showed immediate and almost complete release of the drug substance, ie, 82% in 10 min (Figure 5). All OMZ fibers with ERL or ERS exhibited incomplete drug release. The lowest amount of API (31%) was released from the formulation OMZ_ERL+ERS_7+3. In accordance with literature data, drug release from ERL/ERS-based systems may extend beyond 12 hours.[14,66] For all investigated fibers, Mean Dissolution Time (MDT) and AUC parameters were calculated to quantitatively compare the formulations (Table 2, Figure 9). As expected, the OMZ_PVP formulation had the lowest MDT of 0.12 h and the highest AUC value of 604, due to its high solubility in water. The OMZ_ERS fibers had the longest MDT of 2.23 h and one of the lowest values of AUC, ie, 212. The lowest value of AUC (186) was found in the case of formulation OMZ_ERL +ERS_7+3, which has also long MDT, ie, 1.97 h. While AUC and MDT are often inversely proportional, they describe different aspects of the dissolution profile and are not always directly correlated as dissolution mechanisms are usually complex and depend on many different factors. Such phenomenon has been reported previously in the literature in several studies on the sustained release formulations.[67] El-Masry and Helmy[68] in a study using etamsylate-loaded

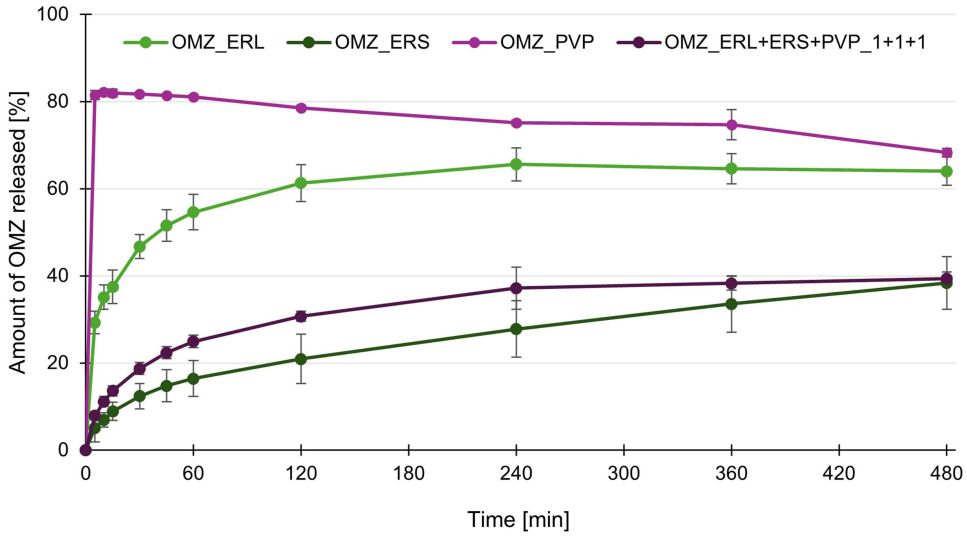

Figure 5 Dissolution profiles of OMZ fibers based on ERL, ERS, and PVP.

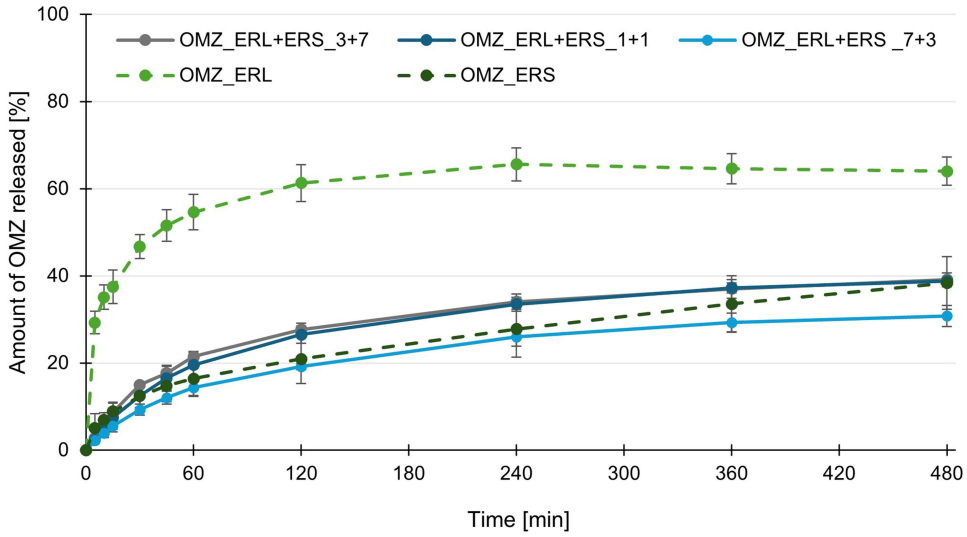

Figure 6 Dissolution profiles of OMZ fibers based on mixtures of ERL and ERS.

hydrophilic hydrogels demonstrated that formulations with similar MDTs exhibited significantly different AUC values over a 12-h period, due to differences in polymer swelling, integrity, and erosion of matrix.[68]

The OMZ_ERL fibers, presented in Figure 5, were characterized by sustained release of the drug substance, reaching 65% at the end of the study. A lower amount of OMZ was released from the OMZ_ERS and OMZ_ERL+ERS+PVP_1+1+1 fibers (38%). Except for the OMZ_PVP fibers, the fastest release of the drug substance was noted in the first 2 hours of testing, ie, burst effect. Following the initial accelerated release of OMZ, a subsequent slowdown in the release rate was observed, which may be attributed to the swelling of the polymer matrix. This swelling likely impedes the diffusion of the drug from within the fiber structure to the surrounding medium. Similar dissolution profiles were reported in the case of ERL/ERS extrudates with flurbiprofen[14] and microneedles with lisinopril dihydrate and ibuprofen based on the Eudragit RL, RS, and ethyl cellulose.[66]

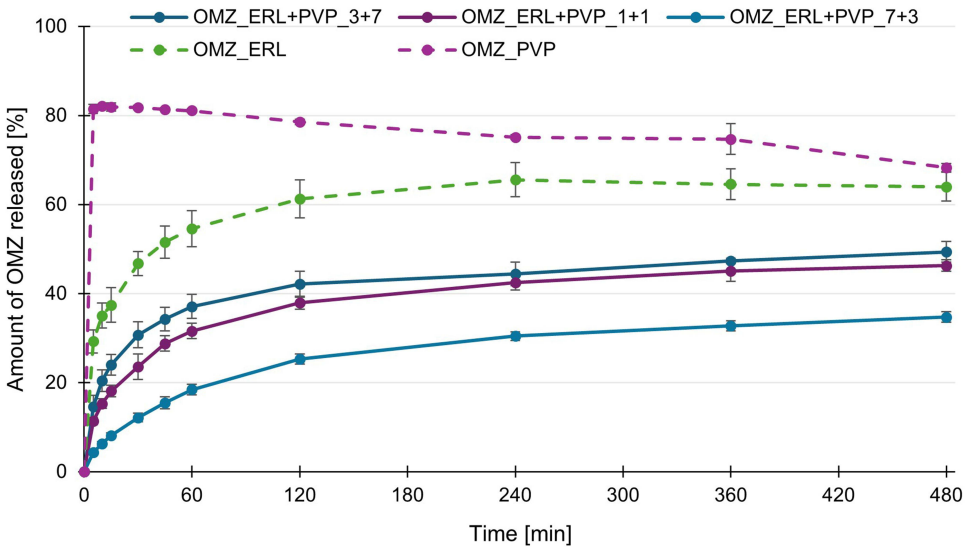

Figure 7 Dissolution profiles of OMZ fibers based on mixtures of ERL and PVP.

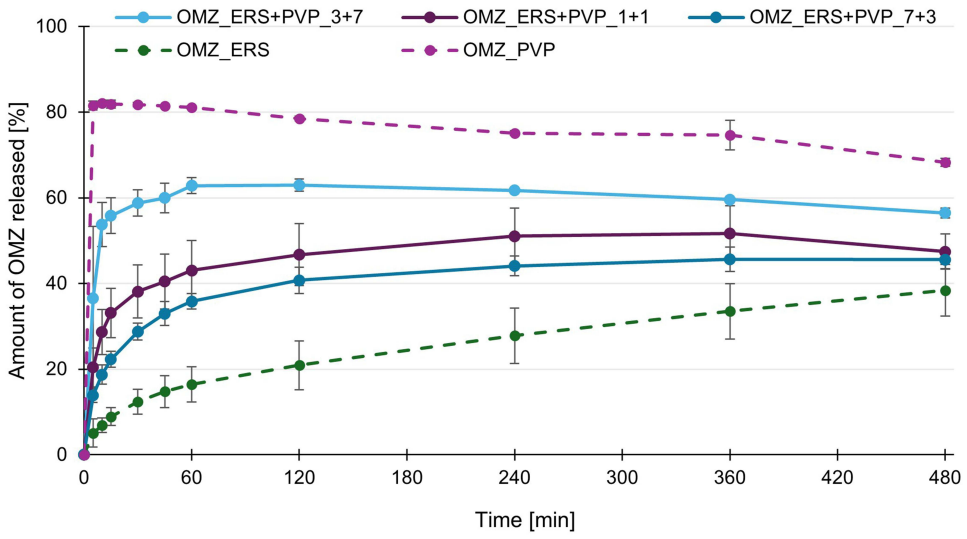

Figure 8 Dissolution profiles of OMZ fibers based on mixtures of ERS and PVP.

The formulations shown in Figure 5 differed significantly from each other in MDT values ($p < 0.05$). The OMZ_ERL +ERS+PVP_1+1+1 fibers had lower MDT values (1.34 h) than OMZ_ERS fibers (2.23 h), due to the presence of highly soluble PVP and ERL with a higher content of quaternary ammonium groups in the polymer structure in the formulation.

Among ERL and ERS-based fibers, the OMZ_ERL+ERS_7+3 formulation was characterized by the lowest amount of OMZ released (31%) (Figure 6). The amount of OMZ released from the fibers containing a lower concentration of ERL was 38%. These observations were opposite to the expected results and the general characteristics of these polymers. ERS features the highest barrier properties, whereas ERL is usually mixed with ERS to increase the permeability of the polymeric matrix.[12] Therefore, ERL-based formulations were expected to have faster API release than ERS-based fibers. Comparing the AUC values for the formulations presented in Figure 6, the OMZ_ERL fibers differed significantly from the other fibers ($p < 0.05$), due to the considerably higher amount of OMZ released. In the case of MDT, additional differences were noted for OMZ_ERS fibers (2.23 h) in comparison to OMZ_ERL+ERS_3+7 and OMZ_ERL+ERS_1+1 fibers (1.69 h and 1.79 h). These differences indicate a faster release of OMZ from the fibers containing up to 49% ERL.

https://doi.org/10.2147/NSA.S535362

Table 2 Comparison of Dissolution Parameters (MDT and AUC) Calculated for OMZ Fibers

Formulation	MDT [h]	AUC
OMZ_ERL	0.58 ± 0.06	486 ± 28
OMZ_ERS	2.23 ± 0.19	212 ± 45
OMZ_PVP	0.12 ± 0.14	604 ± 6
OMZ_ERL+ERS_3+7	1.69 ± 0.09	246 ± 13
OMZ_ERL+ERS_1+1	1.79 ± 0.24	241 ± 13
OMZ_ERL+ERS_7+3	1.97 ± 0.09	186 ± 13
OMZ_ERL+PVP_3+7	1.11 ± 0.13	342 ± 15
OMZ_ERL+PVP_1+1	1.17 ± 0.11	316 ± 14
OMZ_ERL+PVP_7+3	1.67 ± 0.04	220 ± 8
OMZ_ERS+PVP_3+7	0.15 ± 0.04	479 ± 8
OMZ_ERS+PVP_1+1	0.59 ± 0.11	379 ± 48
OMZ_ERS+PVP_7+3	0.76 ± 0.03	331 ± 18
OMZ_ERL+ERS+PVP_1+1+1	1.34 ± 0.05	266 ± 18

Combining ERL and PVP resulted in fibers with a lower amount of OMZ released compared to the OMZ_ERL and OMZ_PVP formulations alone (Figure 7). At the end of the study, 49% and 46% of OMZ were released from the OMZ_ERL+PVP_3+7 and OMZ_ERL+PVP_1+1 fibers, respectively. The fibers containing the lowest amount of PVP were characterized by the lowest amount of OMZ released, ie, 35%. This observation indicates that a high content of PVP in the formulation results in increased release of OMZ, which may be attributed to enhanced matrix permeability. Only the differences in MDT and AUC between OMZ_ERL+PVP_3+7 and OMZ_ERL+PVP_1+1 were not statistically significant ($p > 0.05$).

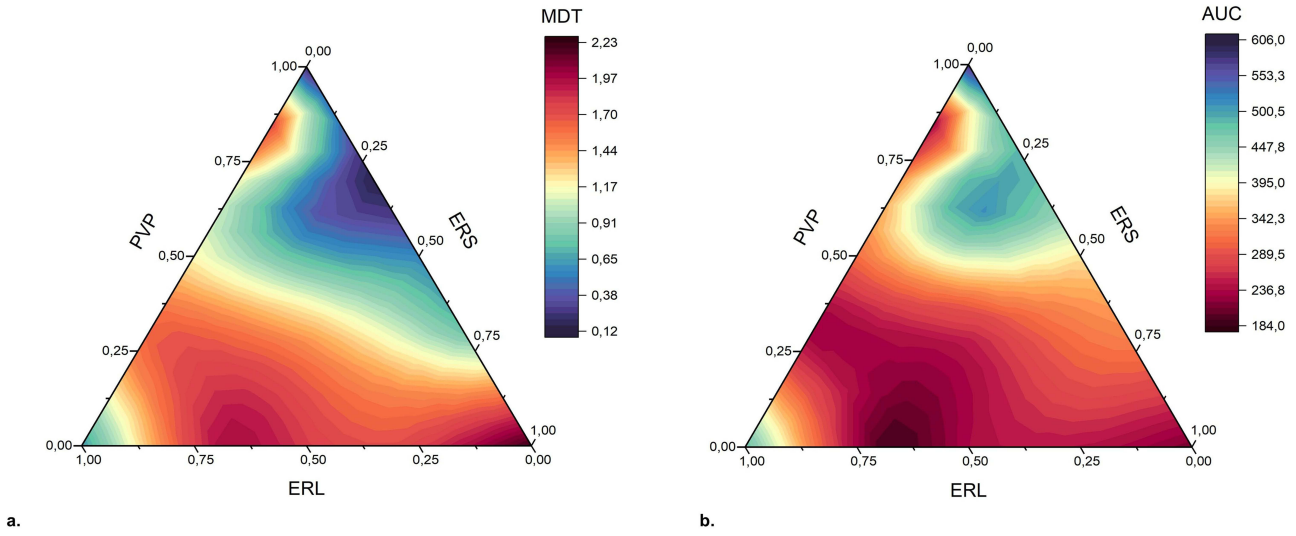

Figure 9 Effect of the composition of OMZ fibers on the dissolution parameters: (**a**) Mean Dissolution Time (MDT), (**b**) Area Under the dissolution Curve (AUC).

As expected, the formulations based on ERS and PVP were characterized by a higher amount of OMZ released than OMZ_ERS fibers (Figure 8). The amount of drug released from the formulation OMZ_ERS+PVP_3+7 was 56% and was the highest among the OMZ_ERS+PVP fibers. It was significantly higher than in corresponding OMZ_ERL+PVP_3+7 fibers ($p = 0.023$). In the case of OMZ_ERS+PVP_7+3 and OMZ_ERS+PVP_1+1 fibers, the amount of the drug released was 46% and 47%, respectively. OMZ_ERS+PVP_3+7 and OMZ_ERS+PVP_1+1 fibers were also similar to each other in AUC and MDT values ($p > 0.05$). In addition, the MDT values for OMZ_ERS+PVP_3+7 (0.15 h) and OMZ_PVP fibers (0.12 h) were not significantly different, indicating similar drug release rates from these formulations.

It was observed that for OMZ_ERL+PVP and OMZ_ERS+PVP fibers, the amount of OMZ released increased with the increasing amount of PVP in the formulation. For OMZ_ERL+PVP fibers, a statistically significant increase in the amount of OMZ released was observed at lower amounts of PVP in the formulation than for OMZ_ERS+PVP. Additionally, OMZ_ERS+PVP fibers were characterized by lower MDT values compared to complementary OMZ_ERL+ERS and OMZ_ERL+PVP fibers ($p < 0.05$).

A gradual decrease in the amount of OMZ released throughout the study was noted for OMZ_ERS+PVP_3+7 and OMZ_ERS+PVP_1+1 fibers. This phenomenon was also observed for OMZ_PVP formulation. It could have occurred as a result of the gradual decomposition of OMZ in the dissolution medium, despite its pH of 7.4. According to the literature, OMZ is stable at pH 7 for 43 h and its stability increases with the increasing alkalinity of the solution to pH 11.[37]

Figure 9 presents the influence of the OMZ fibers composition on MDT and AUC values. With increasing amounts of PVP in the formulation, the MDT is shortened. However, the red area in the upper apex of the triangular graph indicates a nonlinear relationship between these variables. Although the formulation based on ERL alone was characterized by short MDT, combining ERL with ERS significantly decreased the dissolution rate of OMZ. Contrary to MDT, the AUC value increased with the increasing amount of PVP in the formulation.

Bisoprolol Hemifumarate

The results of the dissolution study for BIS fibers are presented in Figure 10 and Table S3. The dissolution curves for the BIS_ERL+ERS_3+7, BIS_ERL+ERS_1+1, and BIS_ERL formulations present a similar dissolution profile, characteristic for the immediate release of API. In the case of these three formulations, the total amount of the API released at the end of the study exceeded 95%. Significantly slower and prolonged release of BIS up to 2h, followed by a plateau phase, was observed for the BIS_ERL+ERS_7+3 formulation. In this case, a total amount of 88% of BIS was released.

The MDT values confirm the immediate release from all BIS-containing fibers (Table 3). The highest value of MDT (0.45 h) was found for BIS_ERL+ERS_7+3 fibers. This value was statistically higher ($p < 0.05$) than for BIS_ERL +ERS_3+7 (0.12 h) and BIS_ERL+ERS_1+1 (0.16 h) fibers. The difference in the MDT between BIS_ERL and

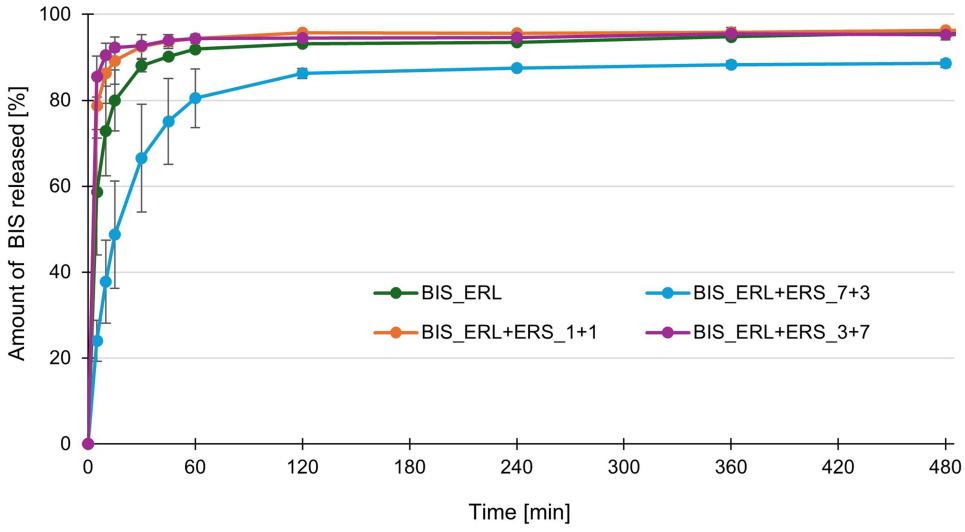

Figure 10 Dissolution profiles of BIS fibers.

https://doi.org/10.2147/NSA.S535362

Table 3 Comparison of Dissolution Parameters (MDT and AUC) Calculated for BIS Fibers

Formulation	MDT [h]	AUC
BIS_ERL	0.29 ± 0.06	738 ± 5
BIS_ERL+ERS_3+7	0.12 ± 0.02	753 ± 10
BIS_ERL+ERS_1+1	0.16 ± 0.04	757 ± 5
BIS_ERL+ERS_7+3	0.45 ± 0.18	669 ± 17

BIS_ERL + ERS_7+3 was insignificant. The lowest AUC value was found for the BIS_ERL+ERS_7+3 fibers (669), and it was significantly different from other BIS fibers ($p < 0.05$).

The release profiles obtained for the BIS and OMZ differ significantly from each other despite the same polymer matrices. The BIS fibers were characterized by the immediate and almost complete release of the drug substance. In contrast, OMZ_ERL+ERS formulations were characterized by sustained release of the drug. The presumed reason for the observed differences might be the interactions between the drug substances and the polymer matrix. OMZ and BIS are small-molecule drugs. OMZ is a lipophilic molecule, whereas BIS has a balanced hydrophilic-hydrophobic characteristic.[37,42] Those properties of drug substances influence their encapsulation efficiency in the polymeric matrix. To achieve the homogenous distribution of the API in the fibrous structure, the hydrophilic drug should be loaded into the hydrophilic matrix, and hydrophobic molecules should be combined with the hydrophobic polymers. The incompatibility between the drug and the polymer can lead to uneven drug distribution in the fibers and its deposition near their outer surface, causing the burst release of the API.[69,70] Positively charged ERL is more hydrophilic than ERS, due to a higher amount of quaternary ammonium groups in its structure.[71] Better BIS compatibility with ERL might explain the slightly slower release of API from BIS_ERL+ERS_7+3 fibers compared to other BIS formulations (Figure 10). Similarly, the OMZ_ERS fibers were characterized by slower API release, than OMZ_ERL fibers, which also might be attributed to the uniform distribution of the drug in the lipophilic polymer matrix (Figure 5). However, this explanation is hardly applicable for OMZ formulations, in which those two polymers are combined.

Other factors influencing the drug release kinetics are process characteristics, drug-polymer charge interactions, solubility, and crystal structure of the drug substance. The blend electrospinning method, applied in this study, contributes to the burst release effect, especially for charged particles. This effect may be further enhanced using small-molecule drugs like BIS, which are characterized by good solubility and are in amorphous form.[1,63,72]

OMZ fibers based on ERL+ERS had higher MDT and lower AUC values compared to respective ERL+PVP and ERS +PVP formulations (insignificant differences in AUC and MDT for OMZ_ERL+ERS_7+3 and OMZ_ERL+PVP_7+3 ($p > 0.05$). This may be related to the overall lower mass of the Eudragit polymers in the PVP-containing formulations, due to the higher concentration of PVP solution used for electrospinning. The addition of PVP, a hydrophilic and neutral polymer, resulted in fibers characterized by sustained release with an initial burst phase.[55] It was expected that the ERL-based fibers would exhibit faster API release because of the high content of hydrophilic moieties that promote polymer swelling.[13] Surprisingly, the ERS+PVP fibers were characterized by a higher amount of OMZ released and a shorter MDT than the ERL+PVP fibers. The observed phenomenon may be due to the larger fiber diameter of ERL+PVP formulations than ERS+PVP. Correlation analysis of the MDT and thickness showed a weak effect of thickness on the values of MDT ($r = -0.34$), but it was without statistical significance ($p = 0.26$). A much stronger dependency was found between thickness and AUC ($r = 0.56$, $p = 0.047$).

Elzayat et al[73] found that the higher the amount of polymer ERS/ERL mixture (1:1) in the formulation and thus the higher the thickness of the diffusion layer, the more sustained the drug release profile.[73] In the case of fibers obtained, their diameter and the ERL/ERS content could also affect the API diffusion time. OMZ_ERL+PVP_7+3 fibers had a diameter of 1.15 µm and an MDT of 1.67 h, while OMZ_ERS+PVP_7+3 fibers had a diameter of 0.54 µm and an MDT of 0.76 h. OMZ_ERL+PVP_3+7 and OMZ_ERS+PVP_3+7 fibers, despite having the largest diameter within the formulation, had the shortest MDTs due to their high PVP content.

The drug release rate from ERL+PVP and ERS+PVP fibers was controlled by the amount of PVP. Among both formulation types, the fibers containing the highest amount of PVP were characterized by the highest OMZ dissolution rate. Akhgari et al[17] developed the electrospun fibers with indomethacin based on ERS and Eudragit S100 (pH-dependent polymer). In pH 7.4, in which ES100 is completely dissolved, the drug release was dependent on its content. It was observed that with an increasing ratio of ES100 to ERS, the indomethacin release was amplified. In contrast, the formulations containing more than 36.5% of ERS were characterized by incomplete drug release after 10 h of the dissolution study.[17] Elzayat et al[73] also found that the amount of drug substance released was lower when increasing the content of ERL and ERS mixture (1:1) in the formulation.[73]

Lastly, the OMZ release from the fibers might also be affected by its lower solubility in the dissolution medium compared to BIS.

Fibers Compression and Minitablets' Assessment

The fibers chosen for minitablets compression were OMZ_ERS+PVP_7+3 and BIS_ERL+ERS_7+3. In the case of fibers with OMZ, the selected formulation had the highest amount of API released from matrices containing two polymers. For BIS, the slowest-releasing formulation was chosen due to its good water solubility.

OMZ fibrous mats had a more brittle and fragile structure than BIS mats, what affected the compression of the fibers (Figure S2). The fibers with OMZ were harder to transfer to the die of the tablet press, due to their crushability when pressed with tweezers. In addition, the sample was less elastic and less prone to compression. More flexible fiber structures based on ERL were better suited for compression due to easier transfer into the die of the tablet press and higher elasticity.

The thickness of the minitablets depended on the compression force applied (Table 4) and it decreased gradually with increasing compression force. Deviation of mass for single unit of the same formulation was below 10% from the theoretical mass.

Dissolution Studies – Minitablets

The results of the dissolution studies for minitablets were compared to the results for the corresponding fibers. None of the minitablets dissolved completely during the studies. It was noted, that mass remaining from the OMZ minitablets were soft and easily disintegrated under low pressure, while the BIS minitablets preserved their shape (Figure S2).

A lower amount of the drug substance was released from OMZ minitablets (40%) than from OMZ_ERS+PVP_7+3 fibers (46%) during 8 h of dissolution studies (Figure 11), but the prolonged release was maintained. The values of the AUC were higher, while MDT was lower for minitablets than for fibers (Table 5).

Similar conclusions were presented in a study by Dave et al[74] in which the effect of compression force on theophylline release from matrix tablets with ERS was investigated. It was observed that the application of compression forces in the range of 4–12 MPa did not affect the release profile of the drug substance from the ERS matrix without the addition of a plasticizer.[74] In another study, it was found that despite the plastic properties, ERS is characterized by better tabletability than ERL.[75]

The amount of BIS released from minitablets was similar as from BIS_ERL+ERS_7+3 fibers (88%). The only exception was minitablets compressed with 250 N, with the higher total amount of API released (Figure 12).

Table 4 Comparison of Thickness and Weight of Minitablets

Formulation	OMZ		BIS	
	Thickness [mm]	Weight [mg]	Thickness [mm]	Weight [mg]
MT_50N	3.41 ± 0.17	16.03 ± 0.60	3.23 ± 0.11	13.55 ± 0.25
MT_150N	2.70 ± 0.12	15.29 ± 0.50	2.55 ± 0.06	13.67 ± 0.24
MT_250N	2.59 ± 0.10	15.20 ± 0.55	2.07 ± 0.15	12.63 ± 0.75
MT_400N	2.41 ± 0.15	14.70 ± 0.79	1.93 ± 0.26	13.48 ± 0.24

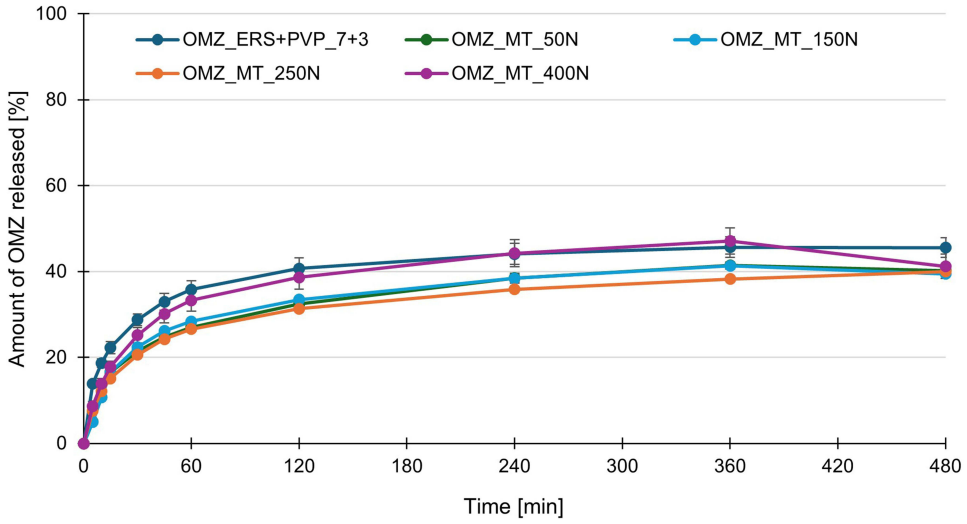

Figure 11 Dissolution profiles of OMZ minitablets.

Dissolution studies showed that BIS release was faster from the MT compressed with the lowest force than from uncompressed fibers (Table 6). The values of MDT were 0.34 h and 0.45 h, respectively. Minitablets compressed with forces of 150 N and 250 N showed similar dissolution rates to fibers. When the highest compression force (400 N) was applied, the dissolution rate was the lowest, and MDT increased to 0.69 h.

The faster dissolution in the case of MT compressed with low force might be caused by the partial breakage of the fibers during compression. On the other hand, when compression force was higher, breaking of the fibers was counterbalanced by their rearrangement and deformation leading to decreased porosity of tablets, which hindered the penetration of water into the tablet matrix and reduced dissolution rate from compressed fibers. It could be confirmed by the slowest dissolution in the case of MT compressed with the highest force.

Elzayat et al[73] reported a slower release of the drug substance with increasing compression force (5–15 kN) from matrix tablets containing a mixture of ERL and ERS (1:1). It was associated with the plastic deformation of Eudragit polymers during compression, which resulted in the formation of hard tablets with low porosity.[73] In the study conducted by Dave et al,[74] a slight but insignificant decrease of the drug release from the ERL and ERS matrices (1:1) was also observed with increasing compression force (4–12 MPa).[74] Eudargit RL and RS are generally characterized by lower compactibility and tabletability than excipients, commonly used for tableting such as microcrystalline cellulose or lactose. Those properties result from their plasticity and axial relaxation upon decompression.[75]

The observed changes in the release profiles of BIS minitablets are more evident than in the case of OMZ minitablets because of the different morphology of compressed fibers. OMZ_ERS+PVP_7+3 fibers were less elastic and more brittle than BIS_ERL+ERS_7+3 fibers.

Table 5 Comparison of Dissolution Parameters (MDT and AUC) Calculated for OMZ Minitablets

Formulation	MDT [h]	AUC
OMZ_ERS+PVP_7+3	0.76 ± 0.03	331 ± 18
OMZ_MT_50N	1.16 ± 0.03	283 ± 7
OMZ_MT_150N	1.09 ± 0.01	284 ± 4
OMZ_MT_250N	1.25 ± 0.04	267 ± 3
OMZ_MT_400N	1.05 ± 0.03	321 ± 22

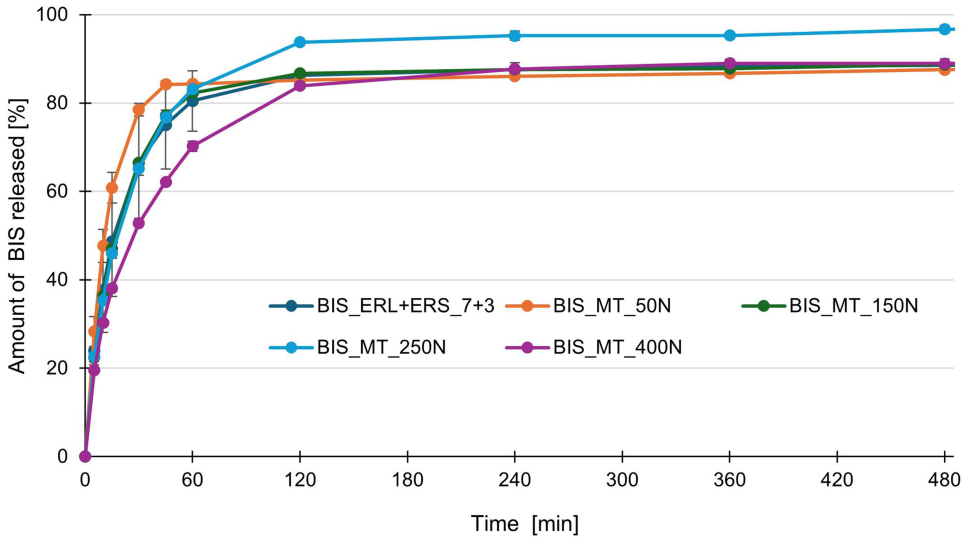

Figure 12 Dissolution profiles of BIS minitablets.

The simplified stability studies for OMZ fibers stored in sealed aluminum bags in a desiccator showed no visual changes in their appearance and no chemical degradation over a 1-year period. In the case of OMZ minitablets stored in plastic containers under room conditions, discoloration was observed, indicating OMZ decomposition after 2 months of storage, particularly in minitablets compressed with forces as high as 250 and 400 N. No change in appearance was observed for BIS fibers and minitablets stored under the same conditions. Unfortunately, all formulations were susceptible to moisture.

Analysis of Release Kinetics

The analysis of the release kinetics performed for the obtained fibers and minitablets with the RKinetDS software showed that for most formulations with OMZ, the best-fitting model was Hopfenberg, indicating an erosive mechanism of drug release. For OMZ_ERS fibers, the best fitting model was Korsmeyer–Peppas, while for OMZ_ERS+PVP_3+7, OMZ_ERS+PVP_7+3, and OMZ_ERL+PVP_7+3 it was Peppas–Sahlin. These models indicate the diffusion-driven drug release kinetics. In the case of OMZ_PVP fibers, it was not possible to collect enough data points with the amount

Table 6 Comparison of Dissolution Parameters (MDT and AUC) Calculated for BIS Minitablets

Formulation	MDT [h]	AUC
BIS_ERL+ERS_7+3	0.45 ± 0.18	669 ± 17
BIS_MT_50N	0.34 ± 0.01	671 ± 3
BIS _MT_150N	0.45 ± 0.04	670 ± 3
BIS _MT_250N	0.54 ± 0.05	717 ± 4
BIS _MT_400N	0.69 ± 0.06	651 ± 6

Abbreviations: OMZ, omeprazole; BIS, bisoprolol hemifumarate; ERL, Eudragit RL PO; ERS, Eudragit RS PO; PVP, polyvinylpyrrolidone, Kollidon K30; MDT, mean dissolution time; AUC, area under the curve; SD, standard deviation.

https://doi.org/10.2147/NSA.S535362

of API released below 65%. Therefore, an analysis without data cutoff (above 65% of API released) was performed, resulting in the best fit with the Peppas-Sahlin model.

While diffusion is the expected release mechanism for ERL- and ERS-based matrices,[13,17,76] only 4 of the 13 formulations exhibited such release kinetics. This may indicate the influence of the polymer type and fiber morphology on the properties of the fiber matrix. The combination of hydrophilic and hydrophobic polymers may have led to matrix perforation due to the rapid dissolution of PVP.[77] Additionally, variations in fiber thickness, increasing the surface-to-volume ratio, could have contributed to erosive kinetics of the drug release.

In comparison to the OMZ_ERS+PVP_7+3 fibers, the best-fitting model for minitablets was Hopfenberg, which indicates an erosive mechanism of API release. The change in release kinetics for this formulation may have occurred as a result of the deformation of inflexible fiber matrix during compression.

In the case of immediate-release BIS fibers, it was necessary to perform the analysis without the data cutoff. The BIS_ERL+ERS_3+7 and BIS_ERL+ERS_7+3 fibers, as well as compressed minitablets were characterized by diffusion-driven drug release mechanisms. The drug substance diffusion from the polymeric matrix may have been enhanced by the good solubility of BIS in water. The best-fitting model for BIS_ERL and BIS_ERL+ERS_1+1 fibers was Hopfenberg, suggesting the erosion-driven release kinetics. In contrast, Glaessl et al[78] observed monotonic and predictable release of metoprolol tartrate by diffusion mechanism from Eudragit RL films. The reason for this phenomenon was the plasticizing effect of the therapeutic substance on ERL.[78]

The obtained results suggest a complex and heterogeneous mechanism of API release from BIS and OMZ formulations.

Conclusion

Thirteen OMZ and four BIS formulations were successfully prepared using ERL, ERS, or PVP. As a result of the electrospinning process, the investigated drug substances transitioned from crystalline to an amorphous form. The morphology of the fibrous mats depended on the drug substance and the polymer content used for the formation of the matrix.

The OMZ formulations exhibited a prolonged release of the drug substance, except for OMZ_PVP fibers. ERL-based formulations were characterized by slower API release than ERS-based fibers, which was the opposite of the Eudragit RL/RS profiles. Increasing PVP content in the formulation led to higher AUC values and OMZ release. Although the same polymeric matrices were used, the BIS nanofibers exhibited immediate and almost complete release of API, except for the BIS_ERL+ERS_7+3 formulation. The latter was characterized by slower, prolonged release of BIS for up to 2 h. After compressing the OMZ_ERS+PVP_7+3 and BIS_ERL+ERS_7+3 nanofibers into minitablets, both maintained the characteristics of sustained drug release. The analysis of the release kinetics indicated an erosive mechanism of drug release for most fibers and minitablets with OMZ. The BIS fibers and minitablets were mainly characterized by diffusion-driven drug release mechanisms, which were expected of Eudragit-based matrices.

The differences in release kinetics between OMZ and BIS fibers may be attributed to their distinct lipophilic and hydrophilic properties, which influenced drug dispersion within the polymer matrix. Additionally, BIS nanofibers had a smaller diameter compared to OMZ fibers, which resulted in a thinner diffusion layer for the drug. Another key factor contributing to the immediate release of BIS from the polymer matrix may be its physicochemical properties, ie, high solubility and an amorphous form.

The limitation of this study is the poor stability of omeprazole observed during dissolution studies, which could be a potential cause of ineffective dose delivery. Further optimization is needed to develop a formulation with a pH maintained at values above 8, which may enhance the stability of the drug substance during dissolution studies. Additionally, the long-term stability of the nanofibers and minitablets will be further examined due to their susceptibility to moisture.

Author Contributions

Conception: JS, EŁ, WB; Study design: JS, EŁ, WB; Execution: JS, EŁ, DM, WB; Acquisition of data: JS, EŁ, DM; Analysis and interpretation: JS, EŁ, DM, WB, AM; Draft preparation: JS; Writing: JS, EŁ, WB; Reviewing and editing:

EŁ, DM, WB, AM; Funding acquisition: JS, WB, AM. All authors made a significant contribution to the work reported, whether that is in the conception, study design, execution, acquisition of data, analysis and interpretation, or in all these areas; took part in drafting, revising or critically reviewing the article; gave final approval of the version to be published; have agreed on the journal to which the article has been submitted; and agree to be accountable for all aspects of the work.

Funding

This research was funded by the Jagiellonian University – Medical College (grant number N42/DBS/000364) and the Faculty of Pharmacy, Jagiellonian University Medical College under the Strategic Program Excellence Initiative at Jagiellonian University (grant number U1C/W42/NO/28.13). The purchase of the equipment has been supported by a grant from the Priority Research Area qLIFE under the Strategic Programme Excellence Initiative at Jagiellonian University, grant number U1C/P04/NO/04.04. DSC measurements were carried out using research infrastructure funded by the European Union in the framework of the Smart Growth Operational Programme, Measure 4.2: Grant No. POIR.04.02.00-00-D001/20, ATOMIN 2.0—Center for materials research on ATOMic scale for the Innovative economy.

Disclosure

Dr Witold Brniak is a member of and reports personal fees from the expert committee of the Polish Pharmacopoeia (Office for Registration of Medicinal Products, Medical Devices and Biocidal Products). It has not influenced this work in any way. The authors report no other conflicts of interest in this work.

References

1. Thakkar S, Misra M. Electrospun polymeric nanofibers: new horizons in drug delivery. *Eur J Pharm Sci*. 2017;107(June):148–167. doi:10.1016/j.ejps.2017.07.001
2. Ahmadi Bonakdar M, Rodrigue D. Electrospinning: processes, structures, and materials. *Macromol*. 2024;4(1):58–103. doi:10.3390/macromol4010004
3. Cho Y, Beak JW, Sagong M, Ahn S, Nam JS, Il-Doo K. Electrospinning and nanofiber technology: fundamentals, innovations, and applications. *Adv Mater*. 2025;2500162. doi:10.1002/adma.202500162
4. Dziemidowicz K, Sang Q, Wu J, et al. Electrospinning for healthcare: recent advancements. *J Mater Chem B*. 2021;9(4):939–951. doi:10.1039/d0tb02124e
5. Feng X, Li J, Zhang X, Liu T, Ding J, Chen X. Electrospun polymer micro/nanofibers as pharmaceutical repositories for healthcare. *J Control Release*. 2019;302(January):19–41. doi:10.1016/j.jconrel.2019.03.020
6. Halim N, Nallusamy N, Lakshminarayanan R, Ramakrishna S, Vigneswari S. Electrospinning in drug delivery: progress and future outlook. *Macromol Rapid Commun*. 2025;46(13):e2400903. doi:10.1002/marc.202400903
7. Wang C, Wang J, Zeng L, et al. Fabrication of electrospun polymer nanofibers with diverse morphologies. *Molecules*. 2019;24(5). doi:10.3390/molecules24050834
8. Luraghi A, Peri F, Moroni L. Electrospinning for drug delivery applications: a review. *J Control Release*. 2021;334:463–484. doi:10.1016/j.jconrel.2021.03.033
9. Yu DG, Li JJ, Williams GR, Zhao M. Electrospun amorphous solid dispersions of poorly water-soluble drugs: a review. *J Control Release*. 2018;292(May):91–110. doi:10.1016/j.jconrel.2018.08.016
10. Nikam A, Sahoo PR, Musale S, Pagar RR, Paiva-Santos AC, Giram PS. A systematic overview of eudragit® based copolymer for smart healthcare. *Pharmaceutics*. 2023;15(2):587. doi:10.3390/pharmaceutics15020587
11. Kajdič S, Planinšek O, Gašperlin M, Kocbek P. Electrospun nanofibers for customized drug-delivery systems. *J Drug Deliv Sci Technol*. 2019;51(January):672–681. doi:10.1016/j.jddst.2019.03.038
12. Patra C, Priya R, Swain S, Kumar Jena G, Panigrahi KC, Ghose D. Pharmaceutical significance of Eudragit: a review. *Futur J Pharm Sci*. 2017;3(1):33–45. doi:10.1016/j.fjps.2017.02.001
13. Thakral S, Thakral NK, Majumdar DK. Eudragit®: a technology evaluation. *Expert Opin Drug Deliv*. 2013;10(1):131–149. doi:10.1517/17425247.2013.736962
14. Mansuroglu Y, Dressman J. Factors that influence sustained release from hot-melt extrudates. *Pharmaceutics*. 2023;15:1996. doi:10.3390/pharmaceutics15071996
15. Jafari-Aghdam N, Adibkia K, Payab S, et al. Methylprednisolone acetate-eudragit® RS100 electrospuns: preparation and physicochemical characterization. *Artif Cells Nanomed Biotechnol*. 2016;44(2):497–503. doi:10.3109/21691401.2014.965309
16. Payab S, Davaran S, Tanhaei A, et al. Triamcinolone acetonide-Eudragit® RS100 nanofibers and nanobeads: morphological and physicochemical characterization. *Artif Cells Nanomed Biotechnol*. 2016;44(1):362–369. doi:10.3109/21691401.2014.953250
17. Akhgari A, Heshmati Z, Afrasiabi Garekani H, et al. Indomethacin electrospun nanofibers for colonic drug delivery: in vitro dissolution studies. *Colloids Surf B Biointerfaces*. 2017;152:29–35. doi:10.1016/j.colsurfb.2016.12.035

18. Mirzaeei S, Taghe S, Asare-Addo K, Nokhodchi A. Polyvinyl alcohol/chitosan single-layered and polyvinyl alcohol/chitosan/eudragit RL100 multi-layered electrospun nanofibers as an ocular matrix for the controlled release of ofloxacin: an in vitro and in vivo evaluation. *AAPS Pharm Sci Tech*. 2021;22(5). doi:10.1208/s12249-021-02051-5
19. Tort S, Han D, Steckl AJ. Self-inflating floating nanofiber membranes for controlled drug delivery. *Int J Pharm*. 2020;579(February):119164. doi:10.1016/j.ijpharm.2020.119164
20. Amarjargal A, Brunelli M, Fortunato G, Spano F, Kim CS, Rossi RM. On-demand drug release from tailored blended electrospun nanofibers. *J Drug Deliv Sci Technol*. 2019;52(April):8–14. doi:10.1016/j.jddst.2019.04.004
21. Omer S, Forgách L, Zelkó R, Sebe I. Scale-up of electrospinning: market overview of products and devices for pharmaceutical and biomedical purposes. *Pharmaceutics*. 2021;13(2):1–21. doi:10.3390/pharmaceutics13020286
22. Vass P, Szabó E, Domokos A, et al. Scale-up of electrospinning technology: applications in the pharmaceutical industry. *Wiley Interdiscip Rev Nanomed Nanobiotechnol*. 2020;12(4):1–24. doi:10.1002/wnan.1611
23. Szabó E, Záhonyi P, Gyürkés M, et al. Continuous downstream processing of milled electrospun fibers to tablets monitored by near-infrared and Raman spectroscopy. *Eur J Pharm Sci*. 2021;164(June):105907. doi:10.1016/j.ejps.2021.105907
24. Celebioglu A, Uyar T. Fast dissolving oral drug delivery system based on electrospun nanofibrous webs of cyclodextrin/ibuprofen inclusion complex nanofibers. *Mol Pharm*. 2019;16(10):4387–4398. doi:10.1021/ACS.MOLPHARMACEUT.9B00798
25. Sipos E, Kósa N, Kazsoki A, Szabó ZI, Zelkó R. Formulation and characterization of aceclofenac-loaded nanofiber based orally dissolving webs. *Pharmaceutics*. 2019;11(8):1–11. doi:10.3390/pharmaceutics11080417
26. Nakamura S, Fukai T, Sakamoto T. Orally disintegrating tablet manufacture via direct powder compression using cellulose nanofiber as a functional additive. *AAPS Pharm Sci Tech*. 2022;23(1):1–11. doi:10.1208/s12249-021-02194-5
27. Pisani S, Friuli V, Conti B, Bruni G, Maggi L. Tableted hydrophilic electrospun nanofibers to promote meloxicam dissolution rate. *J Drug Deliv Sci Technol*. 2021;66:102878. doi:10.1016/J.JDDST.2021.102878
28. Hamori M, Nagano K, Kakimoto S, et al. Preparation and pharmaceutical evaluation of Acetaminophen nano-fiber tablets: application of a solvent-based electrospinning method for tableting. *Biomed Pharmacother*. 2016;78:14–22. doi:10.1016/J.BIOPHA.2015.12.023
29. Partheniadis I, Athanasiou K, Laidmäe I, Heinämäki J, Nikolakakis I. Physicomechanical characterization and tablet compression of theophylline nanofibrous mats prepared by conventional and ultrasound enhanced electrospinning. *Int J Pharm*. 2022;616:121558. doi:10.1016/J.IJPHARM.2022.121558
30. Poller B, Strachan C, Broadbent R, Walker GF. A minitablet formulation made from electrospun nanofibers. *Eur J Pharm Biopharm*. 2017;114:213–220. doi:10.1016/j.ejpb.2017.01.022
31. Nakamura S, Nakura M, Sakamoto T. The effect of cellulose nanofibers on the manufacturing of mini-tablets by direct powder compression. *Chem Pharm Bull*. 2022;70(9):628–636. doi:10.1248/cpb.c22-00290
32. Hellberg E, Westberg A, Appelblad P, Mattsson S. Evaluation of dissolution techniques for orally disintegrating mini-tablets. *J Drug Deliv Sci Technol*. 2021;61:102191. doi:10.1016/j.jddst.2020.102191
33. Klingmann V, Seitz A, Meissner T, Breitkreutz J, Moeltner A, Bosse HM. Acceptability of uncoated mini-tablets in neonates—a randomized controlled trial. *J Paediatr*. 2015;167(4):893–896.e2. doi:10.1016/j.jpeds.2015.07.010
34. Zuccari G, Alfei S, Marimpietri D, Iurilli V, Barabino P, Marchitto L. Mini-tablets: a valid strategy to combine efficacy and safety in pediatrics. *Pharmaceuticals*. 2022;15(1):108. doi:10.3390/ph15010108
35. Filho VJT, Andreazza IF, Sato MEO, Murakami FS. Development of a multiparticulate system containing enteric-release mini-tablets of omeprazole. *Braz J Pharm Sci*. 2014;50(3):505–512. doi:10.1590/S1984-82502014000300008
36. Grzejdziak A, Brniak W, Lengier O, Żarek JA, Hliabovich D, Mendyk A. Application of hydrophilic polymers to the preparation of prolonged-release minitablets with bromhexine hydrochloride and bisoprolol fumarate. *Pharmaceutics*. 2024;16(9):1153. doi:10.3390/pharmaceutics16091153
37. Srebro J, Brniak W, Mendyk A. Formulation of dosage forms with proton pump inhibitors: state of the art, challenges and future perspectives. *Pharmaceutics*. 2022;14(10):2043. doi:10.3390/pharmaceutics14102043
38. Muresan L, Cismaru G, Muresan C, et al. Beta-blockers for the treatment of arrhythmias: bisoprolol – a systematic review. *Ann Pharm Fr*. 2022;80(5):617–634. doi:10.1016/J.PHARMA.2022.01.007
39. European Directorate for the Quality of Medicines & HealthCare (EDQM). Omeprazole, monograph 0942. In *European Pharmacopoeia, Supplement 11.8. Strasbourg, France: Council of Europe*; 2025.
40. European Directorate for the Quality of Medicines & HealthCare (EDQM). Bisoprolol fumarate, monograph 1710. In *European Pharmacopoeia, Supplement 11.8. Strasbourg, France: Council of Europe*; 2025.
41. Bakheit AH, Ali R, Alshahrani AD, El-Azab AS. *Bisoprolol: A Comprehensive Profile*. Vol. 46. 1st. Elsevier Inc.; 2021 doi:10.1016/bs.podrm.2020.07.006
42. El-Masry SM, Helmy SA, Helmy SAM, Mazyed EA. Patient-friendly extemporaneous formulation of bisoprolol: application to stability and bioavailability studies. *Drug Deliv Transl Res*. 2023;13(3):795–810. doi:10.1007/s13346-022-01239-x
43. Charoo NA, Shamsher AAA, Lian LY, et al. Biowaiver monograph for immediate-release solid oral dosage forms: bisoprolol fumarate. *J Pharm Sci*. 2014;103(2):378–391. doi:10.1002/jps.23817
44. Murakami FS, Cruz AP, Pereira RN, Valente BR, Silva MAS. Development and validation of a RP-HPLC method to quantify omeprazole in delayed release tablets. *J Liq Chromatogr Relat Technol*. 2007;30(1):113–121. doi:10.1080/10826070601034485
45. Obajtek N, Mendyk A, Szlęk J, Pacławski A. RKinetDS—Software for Modeling Dissolution Profiles. GitHub. Available from: https://github.com/AleksanderMendyk/RKinetDS_deploy. Accessed July 16, 2025.
46. Podczeck F. Comparison of in vitro dissolution profiles by calculating mean dissolution time (MDT) or mean residence time (MRT). *Int J Pharm*. 1993;97(1–3):93–100. doi:10.1016/0378-5173(93)90129-4
47. Kanjanapongkul K, Wongsasulak S, Yoovidhya T. Investigation and prevention of clogging during electrospinning of zein solution. *J Appl Polym Sci*. 2010;118:1821–1829. doi:10.1002/app
48. De Vrieze S, Van Camp T, Nelvig A, Hagström B, Westbroek P, De Clerck K. The effect of temperature and humidity on electrospinning. *J Mater Sci*. 2009;44(5):1357–1362. doi:10.1007/s10853-008-3010-6
49. Maduna L, Patnaik A. Challenges associated with the production of nanofibers. *Processes*. 2024;12(10):2100. doi:10.3390/pr12102100

50. Marini A, Berbenni V, Pegoretti M, et al. Drug-excipient compatibility studies by physico-chemical techniques: the case of atenolol. *J Therm Anal Calorim*. 2003;73(2):547–561. doi:10.1023/A:1025478129417
51. European Directorate for the Quality of Medicines & HealthCare (EDQM). Atenolol, monograph 0703. *European Pharmacopoeia, Supplement 11.8. Strasbourg, France: Council of Europe*; 2025.
52. Shahabadi SMS, Kheradmand A, Montazeri V, Ziaee H. Effects of process and ambient parameters on diameter and morphology of electrospun polyacrylonitrile nanofibers. *Polymer Sci Series A*. 2015;57(2):155–167. doi:10.1134/S0965545X15020157
53. Cai Y, Gevelber M. The effect of relative humidity and evaporation rate on electrospinning: fiber diameter and measurement for control implications. *J Mater Sci*. 2013;48(22):7812–7826. doi:10.1007/s10853-013-7544-x
54. Park JY, Lee IH, Bea GN. Optimization of the electrospinning conditions for preparation of nanofibers from polyvinylacetate (PVAc) in ethanol solvent. *J Ind Eng Chem*. 2008;14(6):707–713. doi:10.1016/j.jiec.2008.03.006
55. Sebe I, Szabó P, Kállai-szabó B, Zelkó R. Incorporating small molecules or biologics into nanofibers for optimized drug release: a review. *Int J Pharm*. 2015;494(1):516–530. doi:10.1016/j.ijpharm.2015.08.054
56. Kim K, Luu YK, Chang C, et al. Incorporation and controlled release of a hydrophilic antibiotic using poly(lactide-co-glycolide)-based electrospun nanofibrous scaffolds. *J Control Release*. 2004;98(1):47–56. doi:10.1016/j.jconrel.2004.04.009
57. Szabó E, Démuth B, Nagy B, et al. Scaled-up preparation of drug-loaded electrospun polymer fibres and investigation of their continuous processing to tablet form. *Express Polym Lett*. 2018;12(5):436–451. doi:10.3144/expresspolymlett.2018.37
58. Thompson CJ, Chase GG, Yarin AL, Reneker DH. Effects of parameters on nanofiber diameter determined from electrospinning model. *Polymer*. 2007;48(23):6913–6922. doi:10.1016/j.polymer.2007.09.017
59. Rošic R, Kocbek P, Baumgartner S, Kristl J. Electrospun Chitosan/PEO nanofibers and their relevance in biomedical application. *IFMBE Proc*. 2011;1296–1299. doi:10.1007/978-3-642-23508-5_335
60. Murakami FS, Lang KL, Mendes C, Cruz AP, Filho MASC, Silva MAS. Physico-chemical solid-state characterization of omeprazole sodium: thermal, spectroscopic and crystallinity studies. *J Pharm Biomed Anal*. 2009;49(1):72–80. doi:10.1016/j.jpba.2008.10.005
61. Łyszczarz E, Sosna O, Srebro J, Rezka A, Majda D, Mendyk A. Electrospun amorphous solid dispersions with lopinavir and ritonavir for improved solubility and dissolution rate. *Nanomaterials*. 2024;14(19):1569. doi:10.3390/nano14191569
62. Kramarczyk D, Knapik-Kowalczuk J, Kurek M, Jamróz W, Jachowicz R, Paluch M. Hot melt extruded posaconazole-based amorphous solid dispersions—the effect of different types of polymers. *Pharmaceutics*. 2023;15:799. doi:10.3390/pharmaceutics15030799
63. Detrich Á, Dömötör KJ, Katona MT, Markovits I, Vargáné Láng J. Polymorphic forms of bisoprolol fumarate: Preparation and characterization. *J Therm Anal Calorim*. 2019;135(6):3043–3055. doi:10.1007/s10973-018-7553-8
64. Lövgvist K, Sundén G, Noreland D, Ymen I. USOO6150380A. 2000. Available from: https://patents.google.com/patent/US6150380A/en?oq=US+patent+6%2C150%2C380+. Accessed July 16, 2025.
65. Kurakula M, Rao GSNK. Pharmaceutical assessment of polyvinylpyrrolidone (PVP): as excipient from conventional to controlled delivery systems with a spotlight on COVID-19 inhibition. *J Drug Deliv Sci Technol*. 2020;60. doi:10.1016/j.jddst.2020.102046
66. Lammerding LC, Arora A, Braun S, Breitkreutz J. Spatial separation of different drug substances in one microneedle array patch by combining inkjet printing and micromolding technology. *Int J Pharm*. 2025;670. doi:10.1016/j.ijpharm.2024.125102
67. Muhamad H, Mawla N, Dereiah S, Ward A, Williamson J, Asare-Addo K. Comparative analysis of drug release kinetics in polyethylene oxide and xanthan gum matrices with various excipients. *RSC Pharmaceutics*. 2024;2(2):303–317. doi:10.1039/d4pm00296b
68. El-Masry SM, Helmy SA. Hydrogel-based matrices for controlled drug delivery of etamsylate: Prediction of in-vivo plasma profiles. *Saudi Pharm J*. 2020;28(12):1704–1718. doi:10.1016/j.jsps.2020.10.016
69. Zeng J, Yang L, Liang Q, et al. Influence of the drug compatibility with polymer solution on the release kinetics of electrospun fiber formulation. *J Control Release*. 2005;105(1–2):43–51. doi:10.1016/j.jconrel.2005.02.024
70. Hu X, Liu S, Zhou G, Huang Y, Xie Z, Jing X. Electrospinning of polymeric nanofibers for drug delivery applications. *J Control Release*. 2014;185(1):12–21. doi:10.1016/j.jconrel.2014.04.018
71. Naiserová M, Kubová K, Vysloužil J, Bernatonienė J, Brokalakis I, Vetchý D. (Meth)acrylate copolymers of Eudragit® type in oral tablet technology. *Ceská a Slovenská Farmacie*. 2019;68(5):183–197. doi:10.36290/csf.2019.021
72. Karimi Afshar S, Abdorashidi M, Dorkoosh FA, Akbari Javar H. Electrospun fibers: versatile approaches for controlled release applications. *Int J Polym Sci*. 2022;2022. doi:10.1155/2022/9116168.
73. Elzayat EM, Abdel-Rahman AA, Ahmed SM, Alanazi FK, Habib WA, Sakr A. Multiple response optimization of processing and formulation parameters of Eudragit RL/RS-based matrix tablets for sustained delivery of diclofenac. *Pharm Dev Technol*. 2017;22(7):928–938. doi:10.1080/10837450.2016.1212880
74. Dave VS, Fahmy RM, Bensley D, Hoag SW. Eudragit® RS PO/RL PO as rate-controlling matrix-formers via roller compaction: influence of formulation and process variables on functional attributes of granules and tablets. *Drug Dev Ind Pharm*. 2012;38(10):1240–1253. doi:10.3109/03639045.2011.645831
75. Dave VS, Fahmy RM, Hoag SW. Investigation of the physical-mechanical properties of Eudragit® RS PO/RL PO and their mixtures with common pharmaceutical excipients. *Drug Dev Ind Pharm*. 2013;39(7):1113–1125. doi:10.3109/03639045.2012.714786
76. Kakunje S, Badiadka N, Balladka Kunhanna S, et al. Fabrication, characterization and in vitro drug release behavior of electrospun eudragit/eugenol nanofibrous scaffold. *Fibers Polym*. 2024;25(8):2817–2833. doi:10.1007/s12221-024-00622-4
77. Luo Y, Hong Y, Shen L, Wu F, Lin X. Multifunctional role of polyvinylpyrrolidone in pharmaceutical formulations. *AAPS Pharm Sci Tech*. 2021;22:34. doi:10.1208/s12249-020-01909-4
78. Glaessl B, Siepmann F, Tucker I, Rades T, Siepmann J. Deeper insight into the drug release mechanisms in Eudragit RL-based delivery systems. *Int J Pharm*. 2010;389(1–2):139–146. doi:10.1016/j.ijpharm.2010.01.031